CRCLEME
Cooperative Research Centre for
Landscape Evolution & Mineral Exploration

CSIRO
EXPLORATION
AND MINING

AMIRA
Australian Mineral Industries Research Association Limited ACN 004 448 266

OPEN FILE
REPORT
SERIES

THE MINERALOGY AND GEOCHEMISTRY OF SOILS OVERLYING THE BEASLEY CREEK GOLD MINE - LAVERTON, WESTERN AUSTRALIA

Volume 1

I.D.M. Robertson

CRC LEME OPEN FILE REPORT 19

December 1998

(CSIRO Division of Exploration Geoscience Report 105R, 1990.
Second impression 1998)

AMIRA
Australian Mineral Industries Research Association Limited ACN 004 448 266

CRCLEME
Cooperative Research Centre for
Landscape Evolution & Mineral Exploration

CSIRO
EXPLORATION
AND MINING

THE MINERALOGY AND GEOCHEMISTRY OF SOILS OVERLYING THE BEASLEY CREEK GOLD MINE - LAVERTON, WESTERN AUSTRALIA

Volume 1

I.D.M. Robertson

CRC LEME OPEN FILE REPORT 19

December 1998

(CSIRO Division of Exploration Geoscience Report 105R, 1990.
Second impression 1998)

CRC LEME is an unincorporated joint venture between The Australian National University,
University of Canberra, Australian Geological Survey Organisation and CSIRO Exploration and Mining
Headquarters: CRC LEME c/o CSIRO Exploration and Mining, Private Bag, PO Wembley, Western Australia, 6014

RESEARCH ARISING FROM CSIRO/AMIRA REGOLITH GEOCHEMISTRY PROJECTS 1987-1993

In 1987, CSIRO commenced a series of multi-client research projects in regolith geology and geochemistry which were sponsored by companies in the Australian mining industry, through the Australian Mineral Industries Research Association Limited (AMIRA). The initial research program, "Exploration for concealed gold deposits, Yilgarn Block, Western Australia" (1987-1993) had the aim of developing improved geological, geochemical and geophysical methods for mineral exploration that would facilitate the location of blind, buried or deeply weathered gold deposits. The program included the following projects:

P240: Laterite geochemistry for detecting concealed mineral deposits (1987-1991). Leader: Dr R.E. Smith.
Its scope was development of methods for sampling and interpretation of multi-element laterite geochemistry data and application of multi-element techniques to gold and polymetallic mineral exploration in weathered terrain. The project emphasised viewing laterite geochemical dispersion patterns in their regolith-landform context at local and district scales. It was supported by 30 companies.

P241: Gold and associated elements in the regolith - dispersion processes and implications for exploration (1987-1991). Leader: Dr C.R.M. Butt.
The project investigated the distribution of ore and indicator elements in the regolith. It included studies of the mineralogical and geochemical characteristics of weathered ore deposits and wall rocks, and the chemical controls on element dispersion and concentration during regolith evolution. This was to increase the effectiveness of geochemical exploration in weathered terrain through improved understanding of weathering processes. It was supported by 26 companies.

These projects represented "an opportunity for the mineral industry to participate in a multi-disciplinary program of geoscience research aimed at developing new geological, geochemical and geophysical methods for exploration in deeply weathered Archaean terrains". This initiative recognised the unique opportunities, created by exploration and open-cut mining, to conduct detailed studies of the weathered zone, with particular emphasis on the near-surface expression of gold mineralisation. The skills of existing and specially recruited research staff from the Floreat Park and North Ryde laboratories (of the then Divisions of Minerals and Geochemistry, and Mineral Physics and Mineralogy, subsequently Exploration Geoscience and later Exploration and Mining) were integrated to form a task force with expertise in geology, mineralogy, geochemistry and geophysics. Several staff participated in more than one project. Following completion of the original projects, two continuation projects were developed.

P240A: Geochemical exploration in complex lateritic environments of the Yilgarn Craton, Western Australia (1991-1993). Leaders: Drs R.E. Smith and R.R. Anand.
The approach of viewing geochemical dispersion within a well-controlled and well-understood regolith-landform and bedrock framework at detailed and district scales continued. In this extension, focus was particularly on areas of transported cover and on more complex lateritic environments typified by the Kalgoorlie regional study. This was supported by 17 companies.

P241A: Gold and associated elements in the regolith - dispersion processes and implications for exploration. Leader: Dr. C.R.M. Butt.
The significance of gold mobilisation under present-day conditions, particularly the important relationship with pedogenic carbonate, was investigated further. In addition, attention was focussed on the recognition of primary lithologies from their weathered equivalents. This project was supported by 14 companies.

Although the confidentiality periods of the research reports have expired, the last in December 1994, they have not been made public until now. Publishing the reports through the CRC LEME Report Series is seen as an appropriate means of doing this. By making available the results of the research and the authors' interpretations, it is hoped that the reports will provide source data for future research and be useful for teaching. CRC LEME acknowledges the Australian Mineral Industries Research Association and CSIRO Division of Exploration and Mining for authorisation to publish these reports. It is intended that publication of the reports will be a substantial additional factor in transferring technology to aid the Australian Mineral Industry.

This report (CRC LEME Open File Report 19) is a Second impression (second printing) of CSIRO, Division of Exploration Geoscience Restricted Report 105R, first issued in 1990, which formed part of the CSIRO/AMIRA Projects P240 and P241 .

Copies of this publication can be obtained from:
The Publication Officer, c/- CRC LEME, CSIRO Exploration and Mining, PMB, Wembley, WA 6014, Australia. Information on other publications in this series may be obtained from the above or from http://leme.anu.edu.au/

Cataloguing-in-Publication:
Robertson, I.D.M.
The mineralogy and geochemistry of soils overlying the Beasley Creek Gold Mine - Laverton, WA
ISBN v1: 0 642 28290 0 v2: 0 642 28291 9. set: 0 642 28292 7
1. Geochemistry 2. Mineralogy 3. Gold - Western Australia.
I. Title
CRC LEME Open File Report 19.
ISSN 1329-4768

FRONTISPIECE

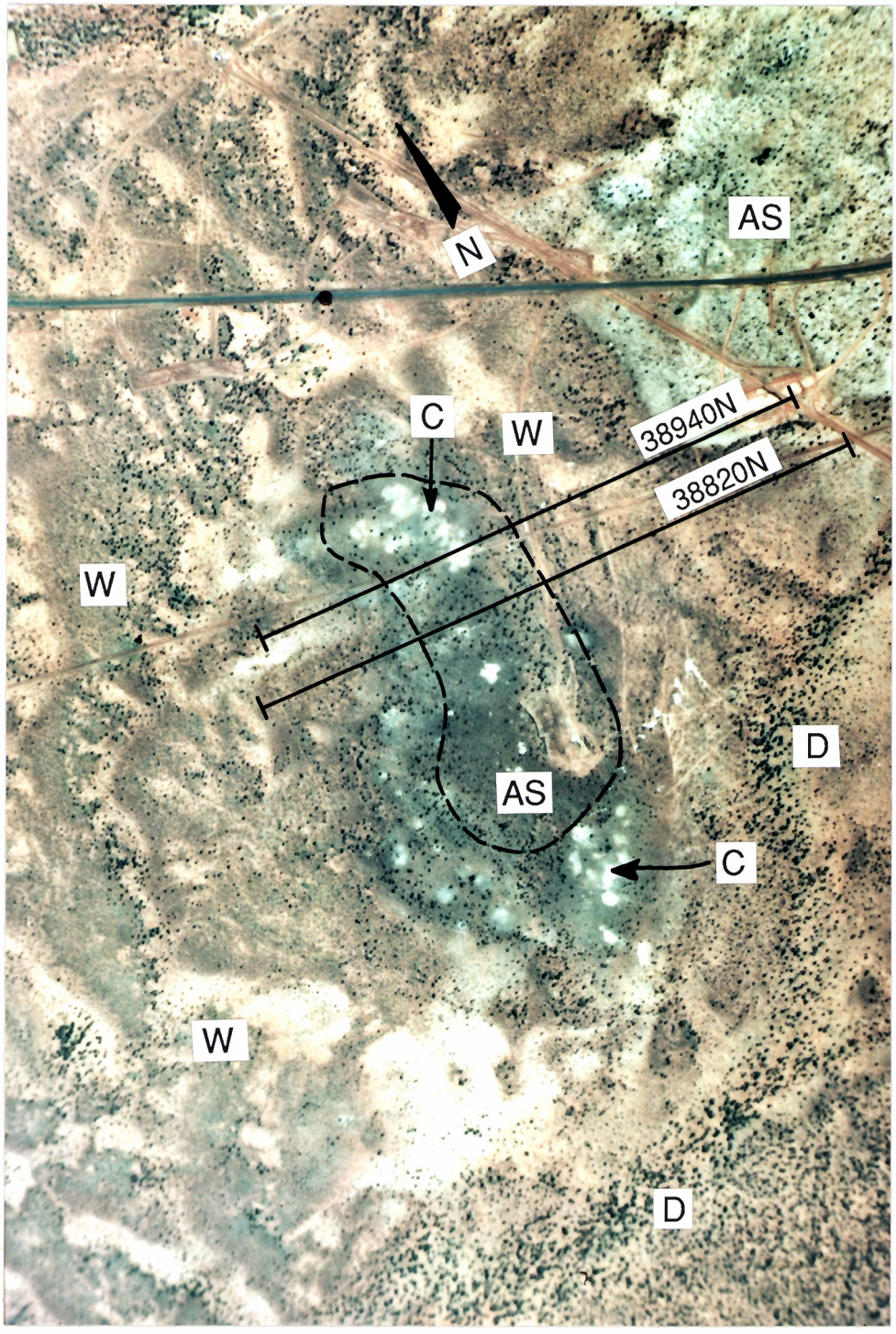

Vertical air photograph of the Beasley Creek Mine Site showing the lag-covered hill of subcropping saprolitic Archaean rocks (AS), surrounded by a wash plain of low Wanderrie banks (W) and a weakly incised broad drainage (D). Patches of calcrete (C) are evident on the hill. The soil traverses and the outline of the pit are also shown. Approximate scale 1 : 13 400. Kevron Aerial Surveys, published with permission of Metex Resources NL.

PREFACE

The CSIRO - AMIRA Research Programme "Exploration for Concealed Gold Deposits, Yilgarn Block, Western Australia" has, as its overall aim, the development of improved geological, geochemical and geophysical methods for mineral exploration that will facilitate the location of blind, concealed or deeply weathered gold deposits.

This report is part of an integrated regolith and bedrock study at Beasley Creek, being carried out jointly by both Module 1 (Laterite Geochemistry, P240) and by Module 2 (Weathering Processes, P241). This report (105R), which describes a mineralogical, petrographic and geochemical study of the soils overlying the Beasley Creek Gold Mine, is part of a series of reports. Others are:-

> A mineralogical, geochemical and petrographic study of the rocks of drillhole BCD 1 from the Beasley Creek Gold Mine - Laverton, WA (MG67R), by Robertson and Gall (1988).
>
> The pre-mining geomorphology and surface geology of the Beasley Creek Gold Mine - Laverton, WA (26R), by Robertson and Churchward (1989).
>
> Geochemistry, petrography and mineralogy of ferruginous lag overlying the Beasley Creek Gold Mine - Laverton, WA (27R), by Robertson (1989).

These reports should be considered together.

The soil and its constituent size fractions have been examined, analysed for 39 elements and assessed as materials suitable for geochemical prospecting. The results show useful anomalies in several pathfinder elements, confirming the results of the previously-reported lag data and provide information on the geological history of the soil components.

The co-operation of Western Mining Corporation Ltd in permitting the early release of this report to the Sponsors of both projects is gently appreciated.

C.R.M. Butt
Project Leader, P241

R.E. Smith
Project Leader, P240

September, 1990.

TABLE OF CONTENTS

LIST OF FIGURES

LIST OF TABLES

1.0 ABSTRACT

Samples of the generally thin soil were collected along two traverses over the Beasley Creek Mine Site, prior to mining. The soil and its components have been examined petrographically, mineralogically and geochemically.

The coarse fraction (710-4000 μm) consists of black, goethite and hematite rich nodules (some of which are magnetic), red to yellow ferruginous clay granules, quartz fragments and scarce fragments of calcrete, hardpan and cellular ironstone. The 710-4000 μm fraction is petrographically indistinguishable from the fine lag which was formed by deflation of the top layers of soil. The fragments of cellular ironstone, which are probably gossanous, are slightly more abundant near the subcrop of the ore.

The black, goethite- and hematite-rich fragments contain lithorelics which have microscopic remnants of muscovite and pseudomorphs after kaolinite, set in, and largely replaced by, massive, spongy or vesicular goethite. The clay-rich granules consist largely of hematite- or goethite-stained kaolinite and some include goethite-rich lithorelics. The soil also contains a significant, quartz-rich, wind-blown component, most abundant in the 75-710 μm fraction, which acts as a geochemical diluent. These subrounded, sand- to silt-sized particles, which include a few grains of fresh microcline, are coated with red iron oxides. The silty fraction (<75 μm) contains less quartz but more iron oxides and clay. The <4 μm fraction is very clay rich.

Sieving and clay sedimentation were used to separate the soil into the 710-4000, the <75 and the <4 μm fractions. The complete soil and its constituent size fractions were geochemically analysed to assess their value as sampling media. The 75-710 μm fraction has a significant component of aeolian sand and was discarded. The distributions of As, Au, Cd, Cu, Sb, Se, W and Zn are related to the occurrence of mineralisation, with anomalies centred over the subcrop of the shales hosting the ore. Maxima in Ca, Mg, P and Sr delineate the calcretes, the P peak being probably related to bone fragments from burrows under the calcrete. The phyllitic ore host rock is indicated by maxima in Ba and Mn and possibly a decrease in Y. The explanation for a maximum in S over the ore and its host rock is problematical.

The complete soil has clearly been diluted by wind-blown sandy material and it is less effective than its fractions as a sampling medium. The most effective medium is the ferruginous 710-4000 μm fraction, followed by the <4 μm clays. The <75 μm silt fraction also contains a significant wind-blown component and is the least effective size fraction.

2.0 INTRODUCTION

A substantial study of the Beasley Creek Gold Deposit, owned by Western Mining Corporation Ltd., is being carried out within the CSIRO/AMIRA Yilgarn Gold Research Programme. This deposit lies about 12 km west north-west of Laverton at 122° 18'E, 28° 34'S. Here, Archaean rocks appear to occupy a small window in the surrounding Permian glacial sediments. The Archaean and Permian rocks have all been deeply weathered. Only the saprolite of the Archaean rocks outcrops in a few places.

Proved and probable ore reserves of 2.1 million tonnes at 2 g/t have been outlined by Western Mining Corp. Ltd. The CSIRO research programme commenced prior to mining, which began at the end of 1987 and had ceased at the time of writing this report.

2.1 CSIRO Work Program

Research being carried out by CSIRO at Beasley Creek comprises studies of the surface geology and geomorphology, the geochemistry of surface materials and the geochemistry of, and dispersions in, the saprolite. Reports have already been issued discussing the geology, geochemistry and mineralogy of the ore zone and footwall rocks (Robertson and Gall, 1988), the pre-mining geomorphology and surface geology (Robertson and Churchward, 1989) and the geochemistry, petrography and mineralogy of the ferruginous lag (Robertson, 1989). This report covers the geochemistry, petrography and mineralogy of the soil. A further report on the surface ironstone, lateritic duricrust, calcrete and ore at shallow depth is in preparation. Geochemical investigation of a section across the deposit from surface to about 80 m depth is in progress and will also be the subject of a future report.

In November 1987, when the mine was at an advanced assessment stage and mining was imminent, the occurrence of surface materials (soil, lag, vein quartz fragments, calcrete, ironstone and saprolite) were mapped and samples of both surface lag and soil were collected along two lines, 38820N and 38940N. Percussion drilling along line 38820N was later sampled to determine dispersion of key elements in the deep saprolite. Samples of ironstone and calcrete were collected over the southern part of the mine site after mining had commenced on the northern part.

2.2 The Potential of Soil Geochemistry at Beasley Creek

The orebody at Beasley Creek was discovered by WMC by soil sampling, and analysis of the coarse fraction (<6.5 mm) for gold. The multi-element geochemical response in this coarse fraction needed to be assessed because Au may not always be anomalous in other circumstances (e.g. leaching). The strength of the anomalies and their degree of dispersion needed to be compared to those of the compositionally similar fine lag. The largely wind-blown, quartz-rich, intermediate fraction was regarded as of little geochemical value. The $<75\,\mu m$ fraction is a commonly-used sampling medium, so it also was selected for a multi-element study. It is suspected that its common use is in part due to its amenability to analysis without further comminution. The included clay fraction contains a significant proportion of iron oxides (hematite and goethite), together with much kaolinite and some very fine-grained quartz. It could, in part, be wind-blown but geochemical evidence suggests that most is probably locally derived from disaggregated lateritic material. Whatever the derivation of the clay fraction, its contained clays and iron oxides are all capable of adsorbing pathfinder elements, which may have been mobile in the landscape. This very fine fraction seemed worthy of particular attention.

3.0 GEOLOGY AND GEOMORPHOLOGY

3.1 Geology

The solid geology, as determined by WMC from percussion drilling, is illustrated in Figure 1A. The orebody lies in a black shale zone, some 15-40 m thick, which dips at 45° to the east. The shale strikes generally north but swings to the west at its southern end and flattens. This black shale unit is intensely weathered to considerable depth (>200 m) and gold is associated with ferruginous zones within it. The black shale is enclosed in a narrow, north-striking mafic amphibolite schist, which is less intensely weathered, particularly where distant from the black shale. The amphibolite schist is in turn enclosed in komatiitic lithologies of the Mt. Margaret Anticline. Small porphyry, granitoid and meta-dolerite lenses intrude the sequence and are associated with north-west striking faults and shears.

3.2 Geomorphology

The geomorphology and surface geology were described by Robertson and Churchward (1989). The Beasley Creek Mine site is on a low hill (Figure 1B), flanked by wash plains consisting of low broad rises or Wanderrie banks, and intervening flat ground (see Frontispiece). The Wanderrie banks are seen as being largely due to unchannelled fluvial flow, although Mabbutt (1963) suggested a significant aeolian contribution. This tract of Wanderrie country forms a low tabular divide above broad drainage floors, in which the channels of ephemeral streams are incised.

The regolith at Beasley Creek has been partly stripped. This is indicated by the absence of a lateritic duricrust over all but the eastern flank of the hill. The western edge of the ferruginous lateritic duricrust closely follows the upper surface of the ore-bearing black shale unit and it seems likely that iron in this unit, probably originally in sulphides, was the source of iron for the lateritic duricrust. Sporadic outcrops of ironstone overlie both the ore-bearing black shale and the meta-dolerites. Extensive calcretes occur near the top of the hill (Figure 1D and Frontispiece). The saprolites of Permian sediments overlap mafic and ultramafic Archaean saprolites in the eastern margin of the pit (Figure 1 A).

3.3 Soil and Soil Components

All the Archaean and Permian rocks at the Beasley Creek mine site are deeply weathered to saprolites and some to lateritic duricrust. The low hill, near the crest of which the phyllitic ore host rock subcrops, is almost completely mantled by residual soil. This soil is thin near the top of the hill (100 mm) and thickens slightly (300-500 mm) on the flanks of the hill and onto the wash plains to the east and west. The base of the soil is generally marked by a substrate of red-brown hardpan, saprolite, hardpan or saprolite with calcrete or calcrete on its own. The soils near the top of the hill are alkaline (pH 8.0-8.5), where calcrete outcrops, but become neutral to acid (pH 5.0-6.5) on the hill flanks and onto the wash plains to the east. Details of soil depths, soil pH, soil texture and the nature of the substrate at the base of the soil are given in Table 1 and shown graphically in Figure 2.

Mechanical analysis shows that the soil contains a wide range of size fractions. The finest is a clay (<4 μm, 2-5% by weight) with a larger proportion of silt (5-75 μm, 10%). The intermediate fraction (75-710 μm) consists largely of wind-blown sand. The coarse fraction (>710 μm) is mainly ferruginous granules (LG201) and pebbles (LG203), using the terminology and codes of Anand *et al* (1989), with minor granules and pebbles of quartz, saprolite and calcrete.

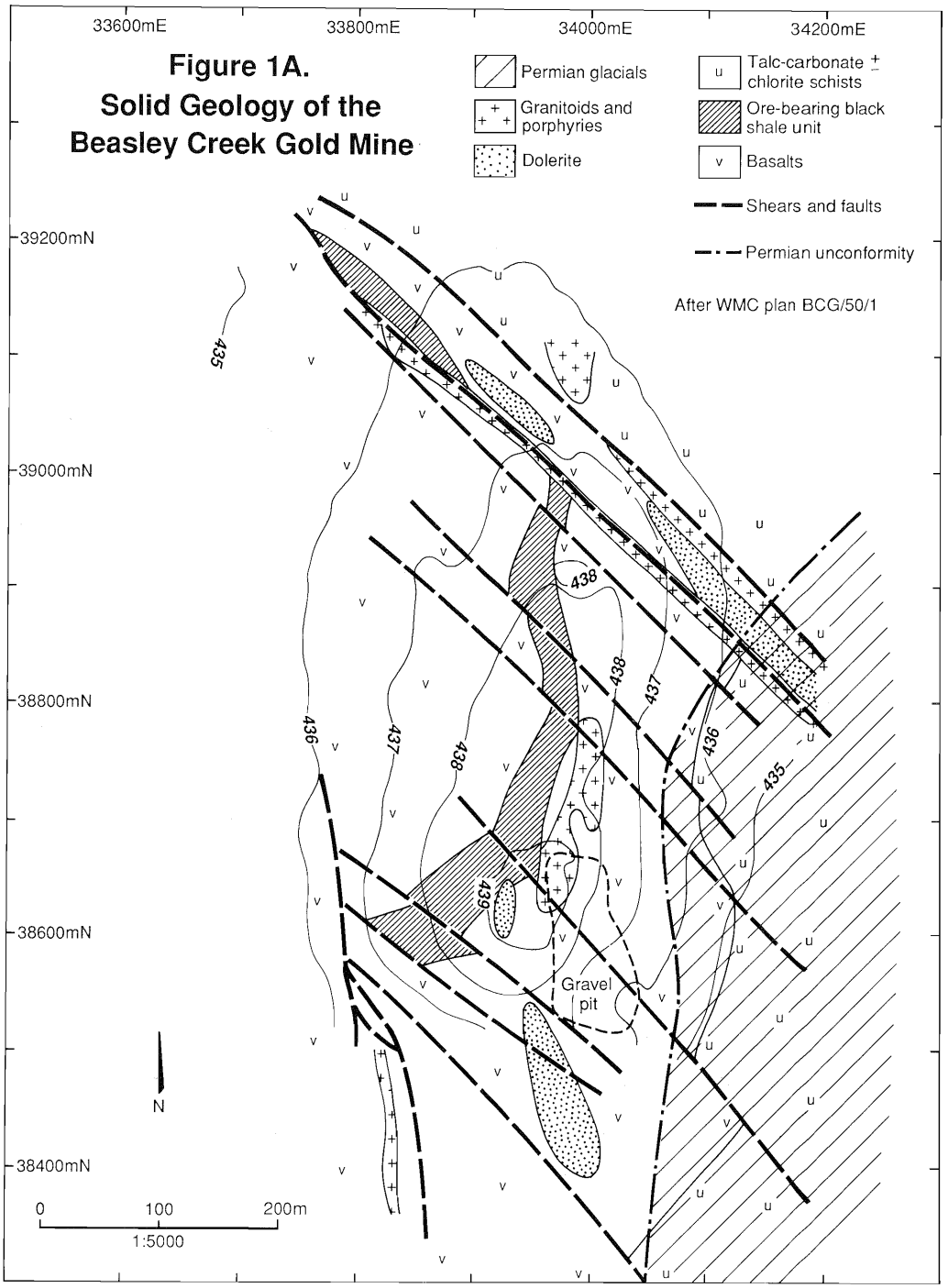
33600mE
33800mE
34000mE
34200mE
Figure 1A.
Solid Geology of the
Beasley Creek Gold Mine
Permian glacials
Granitoids and porphyries
Dolerite
Talc-carbonate ± chlorite schists
Ore-bearing black shale unit
Basalts
Shears and faults
Permian unconformity
After WMC plan BCG/50/1
39200mN
39000mN
38800mN
38600mN
38400mN
435
436
437
438
439
Gravel pit
N
0
100
200m
1:5000

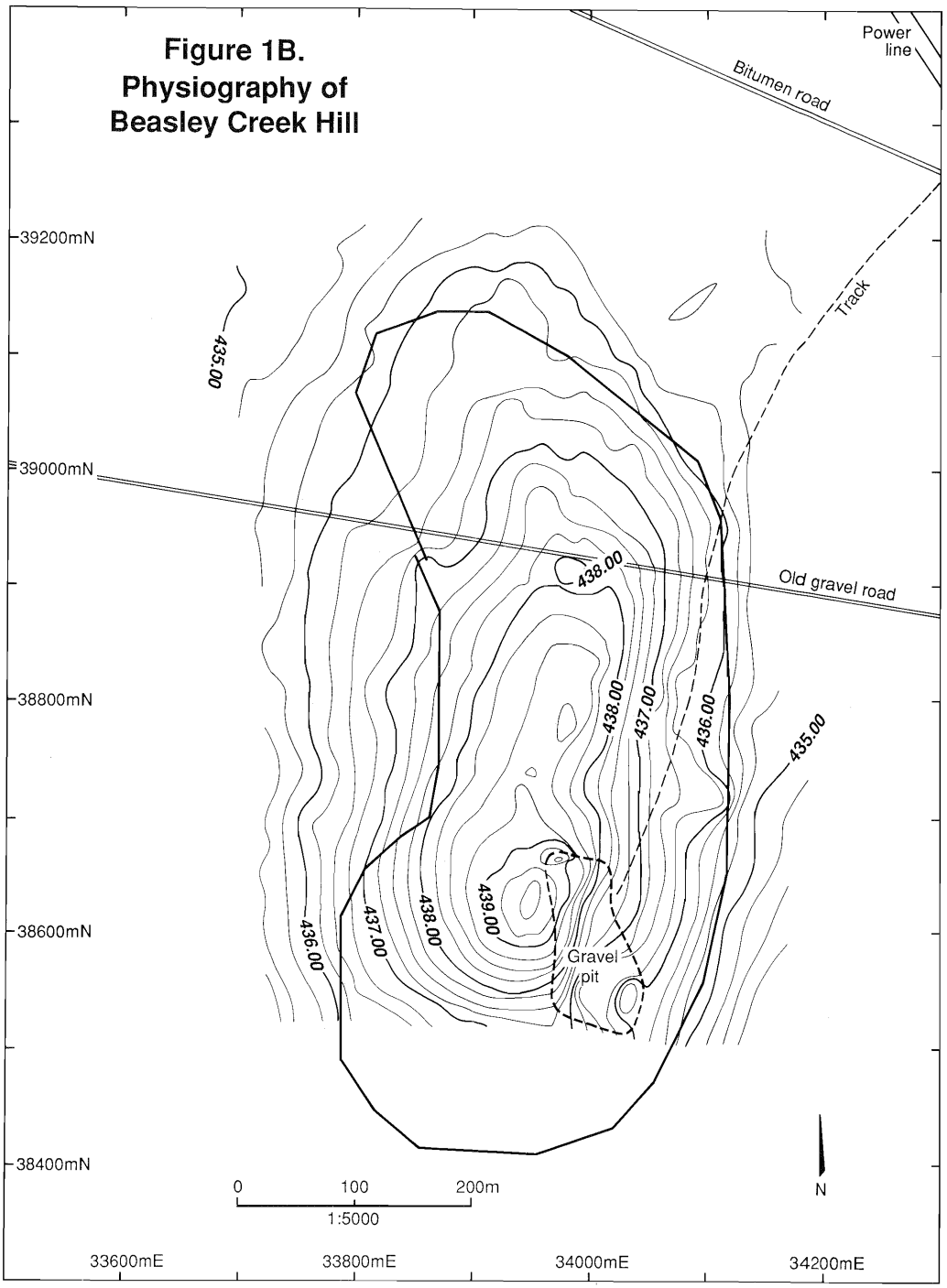
Figure 1B.
Physiography of
Beasley Creek Hill
Power
line
Bitumen road
Track
Old gravel road
Gravel
pit
435.00
436.00
437.00
438.00
439.00
39200mN
39000mN
38800mN
38600mN
38400mN
33600mE
33800mE
34000mE
34200mE
0
100
200m
1:5000
N

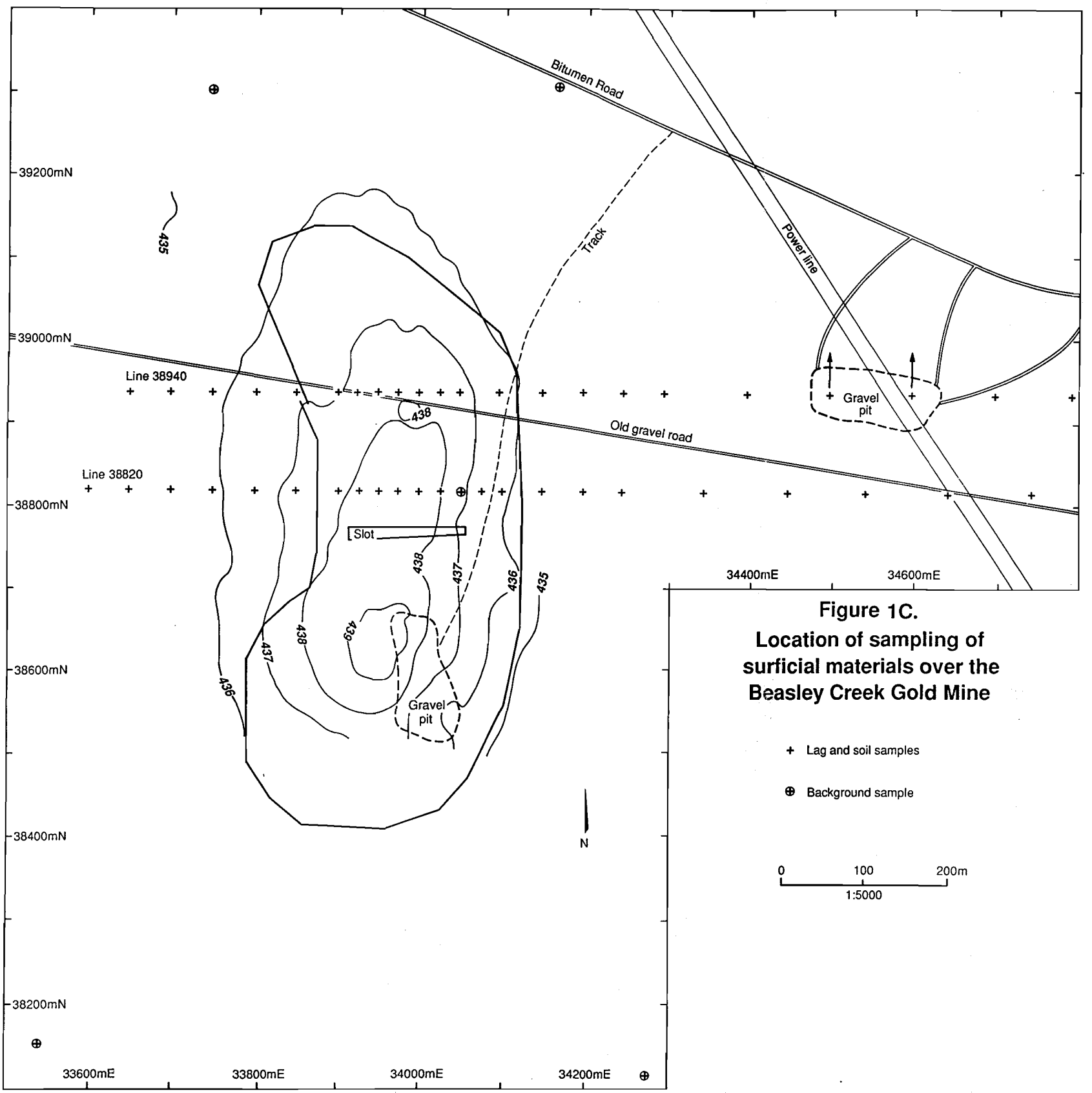

Figure 1C.
Location of sampling of surficial materials over the Beasley Creek Gold Mine

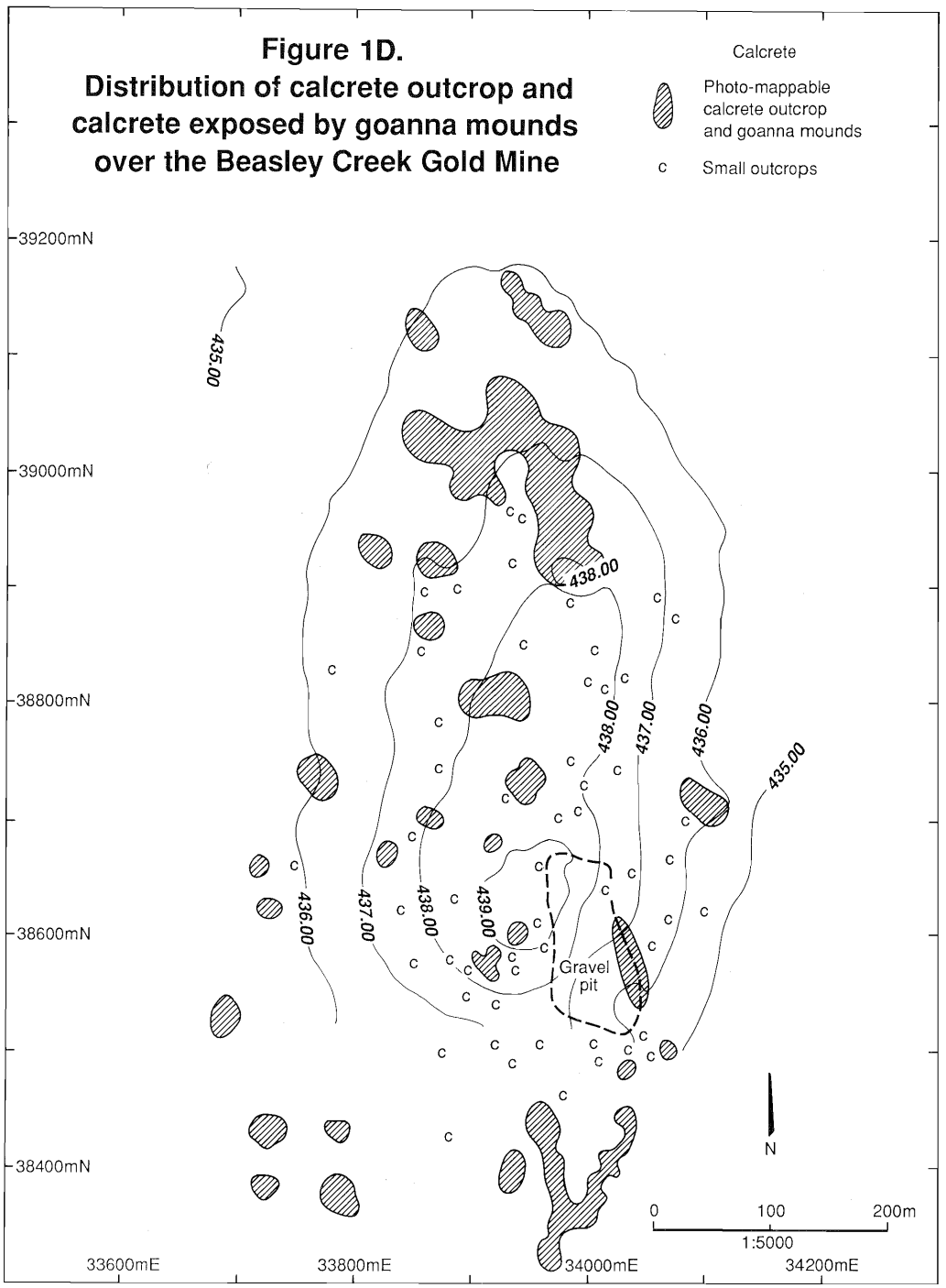
Figure 1D.
Distribution of calcrete outcrop and calcrete exposed by goanna mounds over the Beasley Creek Gold Mine
Calcrete
Photo-mappable calcrete outcrop and goanna mounds
c Small outcrops
39200mN
39000mN
38800mN
38600mN
38400mN
33600mE
33800mE
34000mE
34200mE
435.00
436.00
437.00
438.00
439.00
Gravel pit
N
0
100
200m
1:5000

TABLE 1 - BEASLEY CREEK SOILS

Field No	Easting	Northing	pH	Texture	Depth (cm)	Hard Layer
BC 401	33600	38820	5.0	S L	30	RB Hardpan
BC 402	33650	38820	5.5	C L	35	RB Hardpan
BC 403	33700	38820	5.5	C L	45	RB Hardpan
BC 404	33750	38820	5.5	C L	25	RB Hardpan
BC 405	33800	38820	6.5	S L	15	RB Hardpan + CO3
BC 406	33850	38820	8.0	L C	10	RB Hardpan + CO3
BC 407	33900	38820	6.0	C L	25	Saprolite
BC 408	33925	38820	6.5	S L	10	Saprolite
BC 409	33950	38820	6.5	C L	20	Saprolite
BC 410	33975	38820	6.5	L C	15	Saprolite
BC 411	34000	38820	8.5	C L	10	Saprolite + CO3
BC 412	34025	38820	7.0	C L	15	RB Hardpan + CO3
BC 413	34050	38820	5.0	C L	30	Laterite
BC 414	34075	38820	5.5	L C	50	RB Hardpan
BC 415	34100	38820	5.0	C L	40	RB Hardpan
BC 416	34150	38820	5.0	C L	20	RB Hardpan
BC 417	34200	38820	5.0	C L	30	RB Hardpan
BC 418	34250	38820	5.0	L C	30	RB Hardpan
BC 606	34350	38820	5.0	LC	-	-
BC 607	34450	38820	5.0	SCL	-	-
BC 608	34550	38820	5.0	SLC	-	-
BC 609	34650	38820	5.0	SLC	-	-
BC 610	34750	38820	5.0	SLC	-	-
BC 421	33650	38940	6.0	L C	20	RB Hardpan
BC 422	33700	38940	5.0	L C	20	RB Hardpan
BC 423	33750	38940	5.5	C L	20	RB Hardpan
BC 424	33800	38940	5.5	S L	18	Saprolite + CO3
BC 425	33850	38940	6.0	C L	20	RB Hardpan + CO3
BC 426	33900	38940	6.0	S L	15	RB Hardpan + CO3
BC 427	33925	38940	5.5	S L	10	RB Hardpan
BC 428	33950	38940	8.4	C L	8	Saprolite + CO3
BC 429	33975	38940	8.4	C L	20	CO3
BC 430	34000	38940	8.0	C L	30	CO3
BC 431	34025	38940	5.0	S L	10	Saprolite
BC 432	34050	38940	5.0	L C	30	Laterite
BC 433	34100	38940	5.0	S C L	55	Laterite
BC 434	34150	38940	5.0	S	35	RB Hardpan
BC 435	34200	38940	5.0	L C	20	RB Hardpan
BC 436	34250	38940	5.0	L C	30	RB Hardpan
BC 437	34300	38940	5.0	C L	30	RB Hardpan
BC 601	34400	38940	5.0	SCL	-	-
BC 602	34500	38940	5.0	SCL	-	-
BC 603	34600	38940	5.0	CL	-	-
BC 604	34700	38940	5.0	LC	-	-
BC 605	34800	38940	5.0	LC	-	-
Background Samples						
BC 441	33747	39311	5.0	SCL	-	-
BC 442	34172	39314	5.0	SCL	-	-
BC 443	33545	38146	5.0	SLC	-	-
BC 444	34290	38110	5.0	SLC	-	-

SL= Sandy Loam: CL=Clay Loam: LC=Light Clay: SCL=Sandy Clay Loam: SLC=Sandy Light Clay:

FIGURE 2

Profiles of soil pH, relative levels (R.L.) and soil depths along sample lines 38820N and 38940N. Note the severe vertical exaggeration of the R.L. Horizontal scale in metres.

 Ore body and host rock

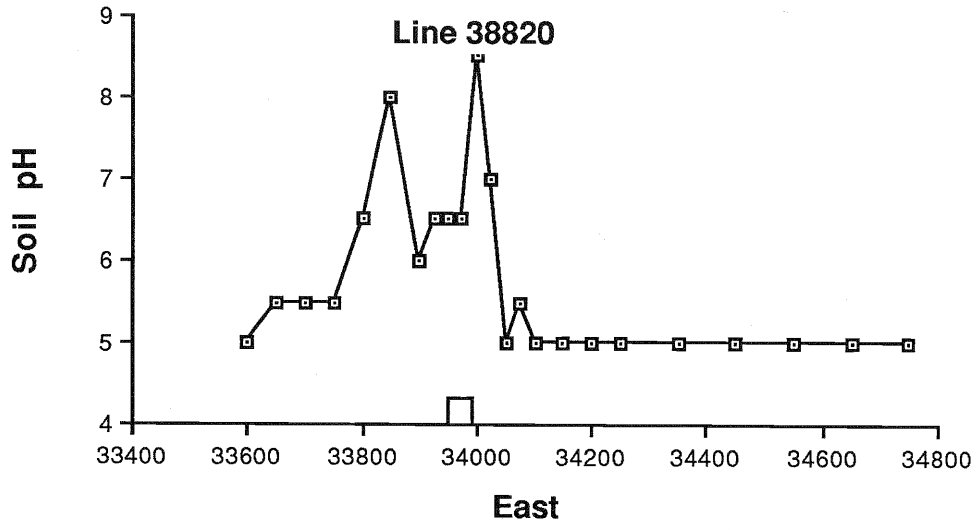
Line 38820
Soil pH
9
8
7
6
5
4
33400
33600
33800
34000
34200
34400
34600
34800
East

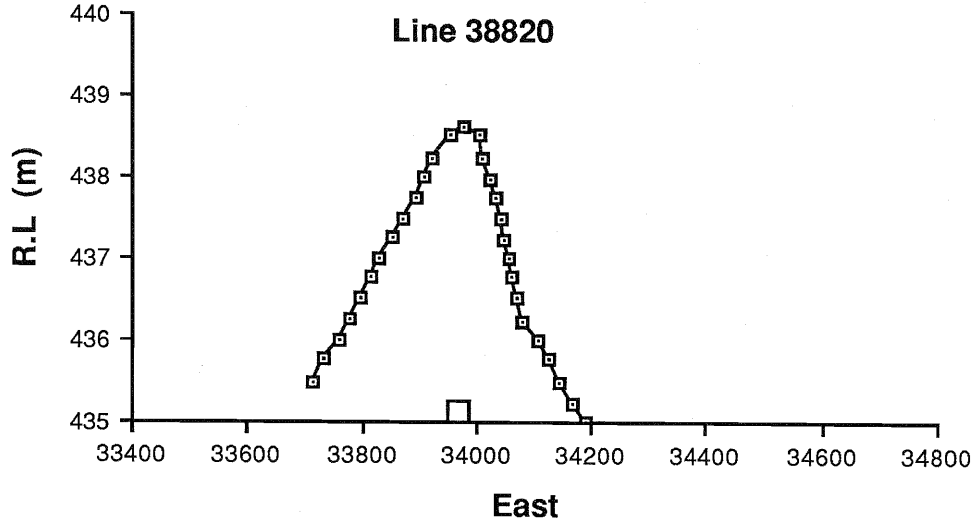
Line 38820
R.L (m)
440
439
438
437
436
435
33400
33600
33800
34000
34200
34400
34600
34800
East

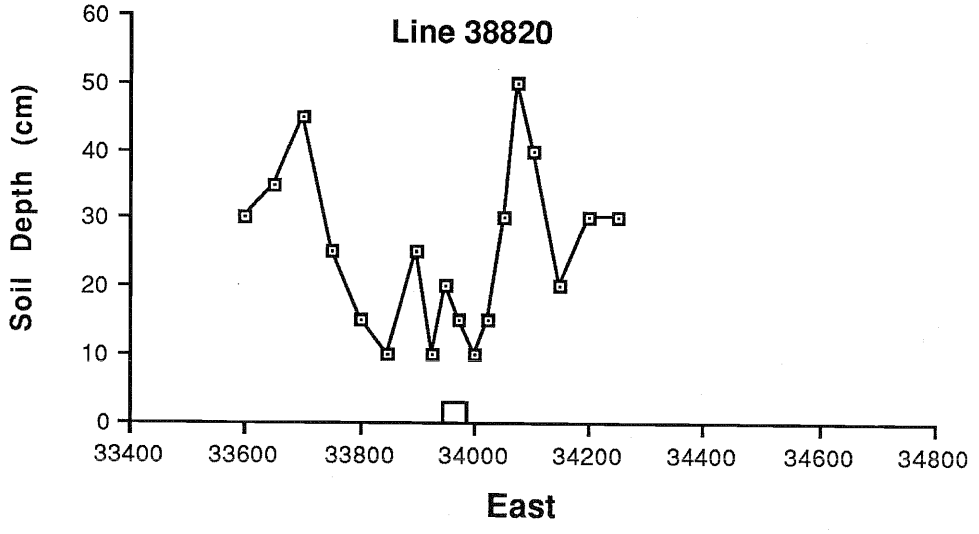
Line 38820
Soil Depth (cm)
60
50
40
30
20
10
0
33400
33600
33800
34000
34200
34400
34600
34800
East

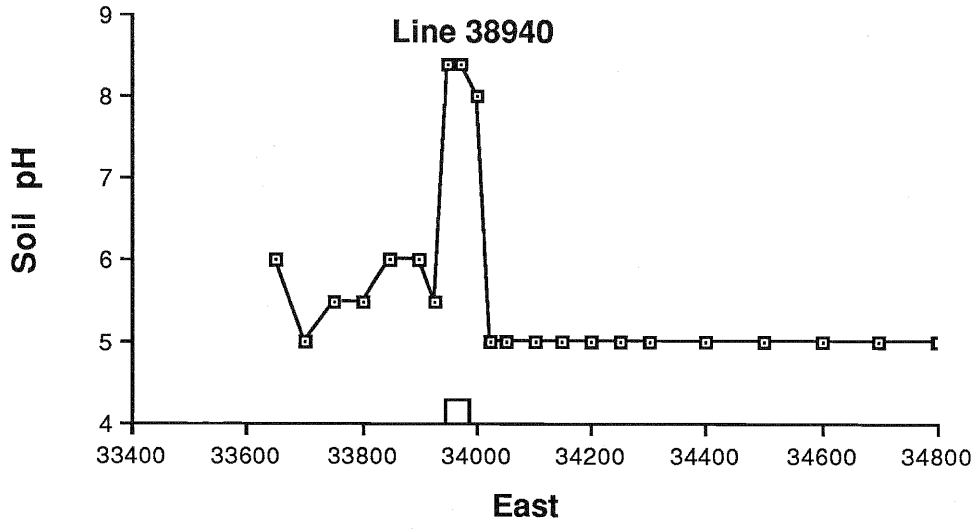
Line 38940
Soil pH
9
8
7
6
5
4
33400
33600
33800
34000
34200
34400
34600
34800
East

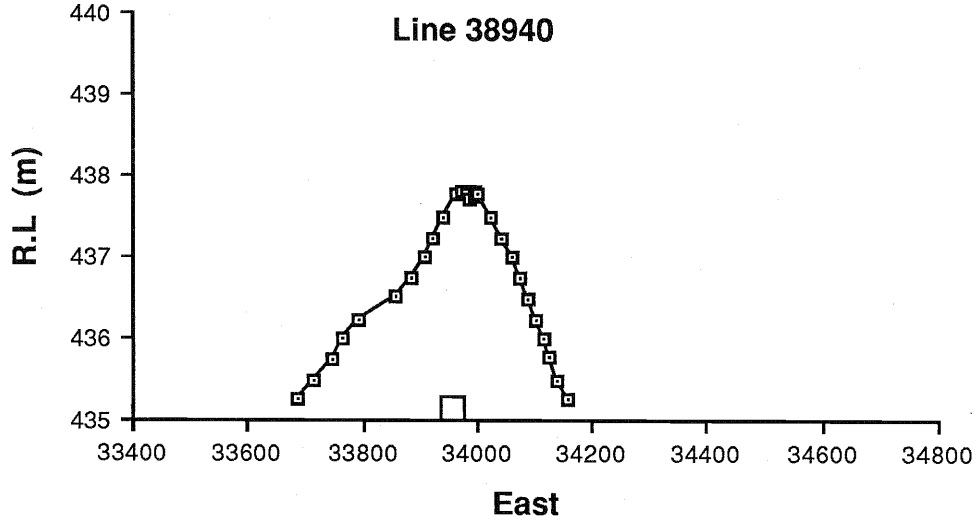
Line 38940
R.L (m)
440
439
438
437
436
435
33400
33600
33800
34000
34200
34400
34600
34800
East

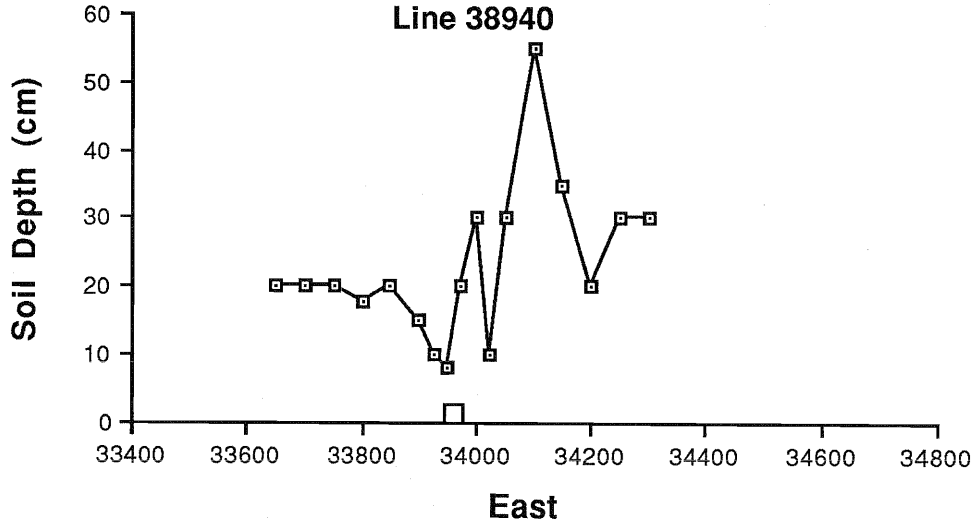
Line 38940
Soil Depth (cm)
60
50
40
30
20
10
0
33400
33600
33800
34000
34200
34400
34600
34800
East

3.4 Aeolian Features

Linear sand dunes, associated with extensive sand planes, provide clear evidence that wind action contributed to the landforms and regoliths within this region. The dunes generally have an east to west orientation, aligned along the trend of the great Australian continental dune swirl (H.M. Churchward, pers. comm.) Dune-forming winds, at this latitude, came from the west. Most of the sand plains are associated with granitic lithologies and, to the east of Laverton, with Permian rocks. In places, such as south of Windarra, sandy lobes extend beyond the granites to cover portions of the greenstone sequence. These sandy portions of the landscape could provide a major source of sand for surrounding areas but they lie some 5 km west of the Beasley Creek Mine site. There are no sand sheets or dunes near the mine site itself. The Wanderrie tracts, which flank the Beasley Creek Mine site, as well as the more distant active fluvial channels (e.g. the Beasley Creek), which drain terrain underlain predominantly by granitic rocks, could also provide sand.

Sand grains, derived from largely granitic alluvium, appear to have moved over the firm surface of the low hill at Beasley Creek, briefly coming to rest between wind storms. Some of this transitory aeolian material then became incorporated in the soil by pedoturbation and illuviation. To this was added ferruginous nodular material, from the underlying saprolites, and clay-rich nodules, from the lateritic duricrust, as well as locally- and distantly-derived clay particles. The sand forms a quantitatively important soil component, where it acts as a geochemical diluent.

Subsequent removal of the sand and the clay, by deflation of the soil surface, has left a thin armour of lag, consisting of fragments of quartz and predominant, black, dense, ferruginous and red-brown, clay-rich granules and nodules. Most are desert varnished and some show dreikanter form (Holmes, 1944). Removal of the coarser, sand-sized particles was probably by a mixture of aqueous transport and by aeolian saltation; the finer sand and silt fractions, and the clay, were transported largely by aeolian action.

3.5 Physiography

A detailed contour map (0.25 m contour interval) was produced by Robertson and Churchward (1989) from WMC natural surface survey data. This contour map is included (Figure 1B) to illustrate the physiography and to assist interpretation of geochemical dispersion patterns in the soils. The hill at Beasley Creek is asymmetrical, with its steeper slope to the east. This steeper slope is preserved by an underlay of hard lateritic duricrust and appears to be maintained by more active erosion at the foot of the hill, due to runoff from the gently undulating terrain to the east. The crest of the hill is partly protected by lateritic duricrust, calcrete (Figure 1D) and surficial ironstone. The phyllitic unit, which contains the orebody, follows the crest of the hill.

4.0 STUDY METHODS

This study necessitated the analysis of 215 samples for 39 elements, some elements being analysed in duplicate by different methods. Also 142 X-ray qualitative and semi-quantitative diffraction analyses were completed. Details of the techniques used for this, the field sampling, fractionation of the soil samples, sample preparation and petrography follow.

4.1 Soil Sampling

Soil samples were collected during a visit in November 1987, when mining was imminent but before the ground was disturbed. The sampling was carried out in conjunction with lag sampling and mapping of the surficial materials (Robertson, 1989; Robertson and Churchward, 1989). Two sample lines were selected,

separated by 120 m (Figure 1C). One line (38820N) passed over the centre of the orebody and the other (38940N) passed over its northern end. The soil samples were collected approximately coincident with lag samples i.e. at 50 m intervals where distant from the orebody and at 25 m intervals over the orebody. At each sample site the upper 25 mm of soil was swept away to remove any contamination from the intensive assessment drilling programme. A small hole 150-250 mm deep was excavated and about 1 kg of soil was removed and bagged in polythene. The hole was then deepened until a hard layer was encountered and the soil depth recorded. The pH and texture of the soil were also recorded. Soil pH was determined in the field using the Universal Indicator from a CSIRO soil pH kit. Soil textures were determined by the standard method of manipulating a handful of soil when moist (McDonald *et al*, 1984).

Background sample sites were selected remote from the orebody, two to the north and two to the south. Their locations are shown in Figure 1C. Preliminary analytical results for Au in the lags indicated that background had not been reached laterally from the orebody. Both the lag and the soil sampling was extended to the east for 500 m on each line to reach background. Here samples were collected at 100 m intervals. It was not possible to extend to the west, as mining had commenced and this area was occupied by the waste dump.

4.2 Size Fraction Analysis

Small subsamples were split from four representative samples, two from points distant from ore and two from near the ore, for preliminary size fraction analysis. The subsamples were first disaggregated by hand and dry sieved on a six sieve stack with brushing. Mesh sizes of 8, 22, 30, 60, 100 and 200 were used. The >8 mesh material was discarded, yielding six size fractions from each sample: 2000-710, 710-500, 500-250, 250-142, 142-75 and $<75\,\mu$m. The $<75\,\mu$m fraction was shaken with a litre of water and allowed to settle overnight. The clay that remained in suspension ($<2\,\mu$m fraction) was siphoned off. This clay, and the sedimented residue (2-75 μm), which still contained some clay, were dried by evaporation. Each fraction was weighed and the percentage yields calculated. All size fractions, except the $<2\,\mu$m fraction, were repeatedly cleaned ultrasonically until the yield of clay was minimal, first in water and then in ethanol, prior to petrographic study.

4.3 Sample Preparation and Clay Fractionation

The size fraction analysis of selected samples, described above, formed part of a pilot study to aid the design of the final soil fractionation scheme. The preparation proceedure for the complete soil sample set is given below.

Lumps in each soil sample were broken by hand until the sample passed a 4 mm screen. Vegetable matter and any large stones were rejected. The sieved soil was split into four parts, using a PVC riffle splitter. One part was retained for reference, one was milled in a case-hardened steel mill and submitted for analysis as a whole. The remaining two parts were combined and this subsample separated into three components, as shown below, and each analysed separately.

The subsample was dry sieved in nylon and polystyrene for 20 minutes on an International Cumbustion Ro-Tap sieve shaker. Three size fractions were collected (710-4000, 75-710 and $<75\,\mu$m). All fractions were shaken with de-ionised water to which a few drops of analytically pure, concentrated NH_4OH had been added to disperse any adhering clay-sized particles. Both the 710-4000 and the 75-710 μm fractions were subjected to ultrasonic agitation. The clay-bearing liquid was decanted through a $75\,\mu$m screen and added to the $<75\,\mu$m fraction. After several changes of water and ultrasonic treatment, the clean 710-4000 μm fraction, rich in ferruginous granules, was dried at 95° C and the sandy 75-710 μm fraction was discarded. This rather involved method (Figure 3A) was necessary in order to maximise the yield of clay

in order to obtain sufficient for analysis. The clay separation method could have been considerably simplified if a larger soil sample (>3 kg) had been collected (Figure 3B).

The <75 μm suspension was made up to 3.5 litres with de-ionised water. Analytically pure, concentrated NH_4OH was added dropwise, until a pH of 8.0 (measured by pH meter) was achieved, to disperse the clays. The suspension was allowed to settle for 20 minutes through a depth of 100 mm. At this stage, only particles <9 μm would still be in suspension (Stokes Law). Most of the suspension (>95%) was decanted using a specially constructed PVC siphoning tube. The <75 μm sediment, from which most of the clay had been removed, was dried at 95° C, disaggregated in agate and packaged for analysis.

The clay-rich suspension was acidified dropwise with analytically pure, concentrated HCl to a pH of 4.0, to flocculate and precipitate the clays. Some samples consumed a little more acid than others. In these, the pH tended to stabilise at pH 6-7, apparently due to the buffering effect of minor calcite and, on addition of further HCl, the pH finally decreased to 4.0. After settling for 30 minutes, the overlying liquid was withdrawn and the clay floc dried at 95° C and disaggregated by hand in agate prior to analysis. Despite adequate drying, the clays tended to 'ball' and stick to the agate surfaces.

Clay dispersion, using NH_4OH, significantly improved the yield of clay and was considered to be far less likely to contaminate than technical grade polyphosphate (e.g. tetra sodium pyrophosphate), which would normally be used for this purpose. The short exposure (about one hour) of the clays to a pH range of 4.0-8.0, which is not extreme in the natural environment, and the use of pure water and reagents, was not regarded as likely to have significantly modified the clay chemistry, though carbonates would be dissolved. Clay flocculation at pH 4.0 was far quicker and more efficient than centrifugal separation of the dispersed clay.

Clay sedimentation was carried out only once on the <75 μm fraction, so it is inevitable that some clay still remained in the <75 μm material. Clay separation using this technique is approximate. Stokes law assumes spherical particles, laminar flow and requires accurate values for the viscosity of the fluid and the densities of both fluid and particles. Clay particles are platelike and the clays contain an appreciable component of attached iron oxides, so varying their densities, fluid dynamics and hence settling velocities. To test the product of clay sedimentation, a few mg of the clay was dispersed in dilute NH_4OH and the dispersion evaporated on a glass slide. This was coated with carbon and gold and examined by SEM. It showed a mass of clay platelets, aligned to the plane of the slide, and demonstrated that most particles were 1 μm or less in size, with a few reaching three to four microns. A very few 10-12 μm plates were found. It would be fair to describe the clay fraction as nominally <4 μm (i.e. >95% are <4 μm).

4.4 XRD Analysis

Qualitative Analysis

All the complete soil samples and all the <4 μm fraction samples were examined by X-ray powder diffractometry at Floreat Park. A Philips PW1050 diffractometer was used, fitted with a graphite crystal diffracted beam monochromator. CuKα radiation was used for both qualitative and semiquantitative analysis. Each sample was scanned over the range 5-65° 2θ at a speed of 1° 2θ/min and data were collected at 0.02° 2θ intervals. Mineralogical compositions were determined by comparison with JCPDS files and laboratory standards. The complete soil samples were examined by using the boric acid-backed pressed discs used for XRF analysis. Diffusion of boric acid through the sample from the backing gave extraneous peaks which were ignored during interpretation. The <4 μm fraction samples were examined using glued, self-supporting XRF discs. The results are tabulated in Appendix 9.

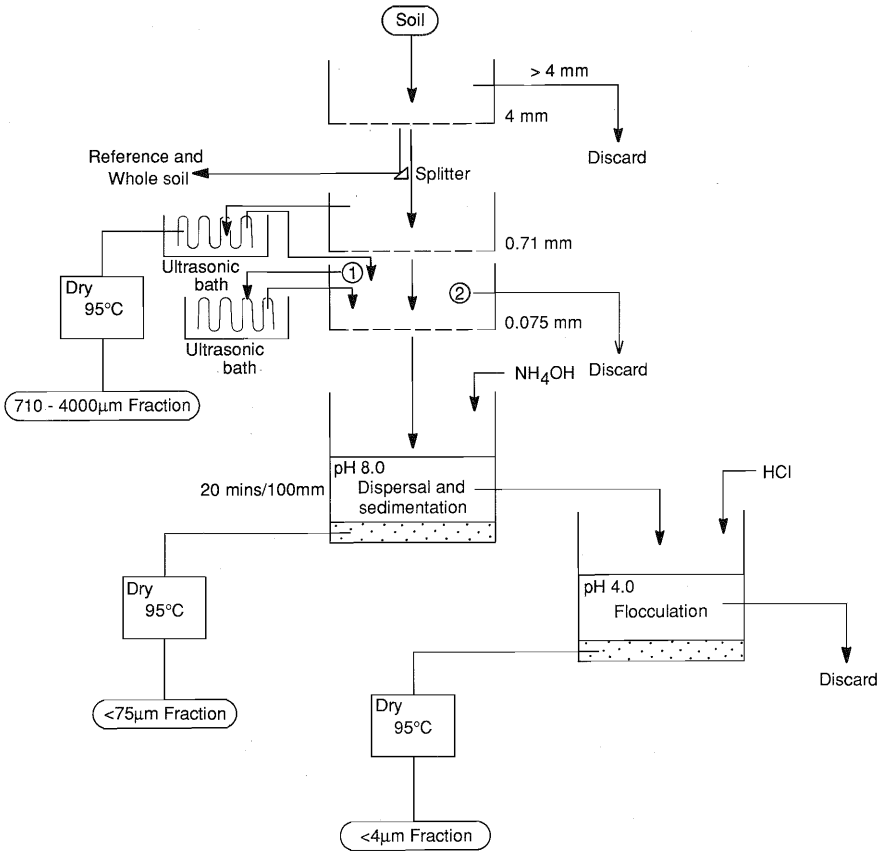

Figure 3A
Sample preparation flow chart.

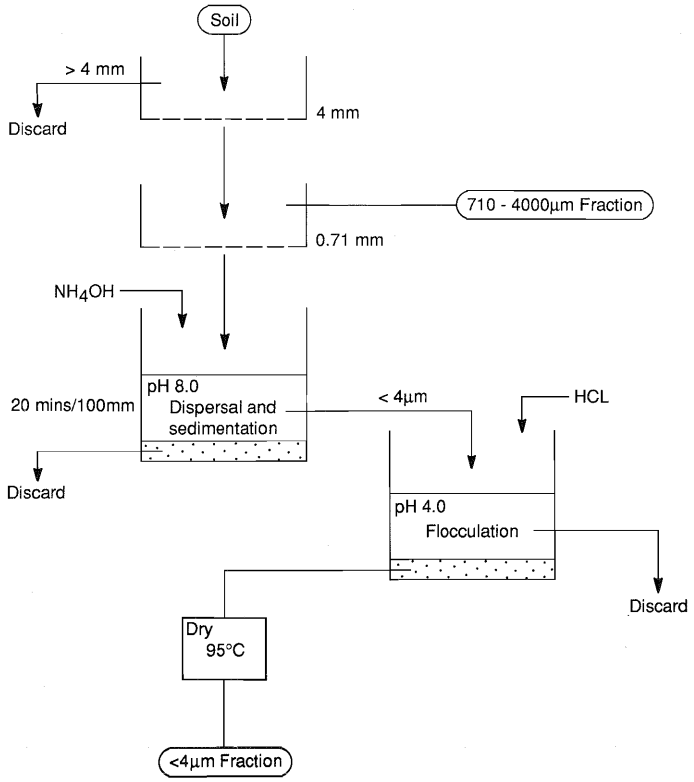

Figure 3B
Simplified soil fractionation flow chart.

A smaller subset of coincident samples, of the complete soil and of each size fraction (710-4000, <75 and <4 μm) were analysed at North Ryde using a Philips PW1729 generator, fitted with a PW1820 vertical goniometer with a graphite crystal monochromator. Each pulped sample, mounted in an Al holder, was scanned, using CuKα radiation, over the range 2.5-67° 2θ and data were gathered over 0.03° 2θ steps. Each step was counted for 1 second, giving a scan rate of 33.3 secs/° 2θ. The results are tabulated in Appendix 8.

Semi-quantitative estimation of mineral abundances

Mineral abundances were estimated using the height above background of a selected XRD peak for each mineral (Table 2). The measured peaks were chosen so as to avoid overlap by peaks of other minerals. It must be emphasised that these results are approximate and are influenced by the degree of crystallinity, mass absorption of the sample and mineral orientation as well as by abundance. The major element geochemistry (Appendices 1 and 2) shows that there is a wide variation in the Fe content of the soil fractions, particularly between the ferruginous 710-4000 μm fraction and the siliceous fine fractions. For XRD mineralogical comparisons to be meaningful, it was therefore necessary to take into account the mass absorption of abundant elements of high atomic number. The method of Brindley (1980) was employed. All major elements were used, including Ti, to calculate the mass attenuation coefficient which in turn was used to correct the measured peak heights. Though all data are in arbitrary units, they give a rough comparison of the relative abundances of *particular* minerals *between* samples; they do not indicate the relative abundances of the different minerals in each sample.

TABLE 2
DIFFRACTION PEAKS USED FOR
SEMI-QUANTITATIVE MINERALOGY

Mineral	Diffraction peak (hkl)	d-Spacing (Å)
Quartz	101	3.34
Microcline	002	3.24
Sericite	002	9.97
Kaolinite	001	7.10
Calcite	002	3.03

4.5 Geochemical Analysis

Detection limits and methods used for the analysis of each trace element are given in Table 3. Neutron activation analysis was by Becquerel Laboratories on 30 g aliquots, except for the <4 μm fraction, where approximately 10 g was used, due to scarcity of material. Minor and trace elements were determined on pressed discs, using a Philips PW1220C XRF at Floreat Park, by the methods of Norrish and Chappell (1977) and Hart (1989). Iron was determined on pressed powder samples, for matrix correction, and these results are included. Sodium data was also gathered from pressed powder samples. Though fused discs would have provided a lighter and simpler matrix and the particle effect would have been eliminated, these data, with a detection limit of 0.05% Na_2O are more reliable than those obtained from our ICP, where Na analysis of materials of <0.6% Na_2O has a very poor precision. Major elements and some minor elements were also determined at Floreat Park by ICP analysis on a Hilger E-1000, after Li-metaborate fusion. Their precision is not as good as may be expected from fused disc XRF analysis but it is generally acceptable.

TABLE 3
TRACE ELEMENT
DETECTION LIMITS AND METHODS

Element	Det. Limit (ppm)	Method
Ag	0.1	ICP/MS
As	2	INAA
Au	0.005	INAA
Ba	15, 100	XRF, ICP
Be	5	ICP
Bi	0.1	ICP/MS
Cd	0.05	ICP/MS
Ce	2, 10	INAA, XRF
Co	1	INAA
Cr	5, 100	INAA, ICP
Cu	5, 100	XRF, ICP
Ga	5	XRF
Ge	3	XRF
In	0.05	ICP/MS
La	0.5	INAA
Mn	20, 100	XRF, ICP
Mo	5	INAA
Nb	5	XRF
Ni	10, 50	XRF, ICP
Pb	5	XRF
Rb	5	XRF
Sb	0.5	INAA
Se	2	XRF (lc x5)
Sn	0.1	ICP/MS
Sr	3	XRF
V	10, 100	XRF, ICP
W	2	INAA
Y	3	XRF
Zn	5	XRF
Zr	4, 100	XRF, ICP

INAA - Instrumental Neutron Activation Analysis - Becquerel Laboratories
XRF - X-ray Fluorescence Analysis - CSIRO, Floreat Park
ICP - Inductively Coupled Plasma Spectrophotometry - CSIRO, Floreat Park
ICP/MS - Inductively Coupled Plasma Mass Spectrometry - Analabs, Perth
lc - Long counting technique

Five characteristically low-level elements, Ag, Cd, In, Sn and Bi, were determined by ICP/MS at Analabs, Perth. A total of 200 mg of each sample was dissolved in hot HCl. HF and $HClO_4$ were added and the whole evaporated to dryness. The sample was taken up in concentrated HCl and made up to 20 ml. An aliquot of 1 ml of this stock solution was diluted with a further 9 ml of 10% HCl before presentation to the ICP/MS. Below 7.5 ppm, Ag remains soluble.

The Ag data seem a little high; a background of 0.1 ppm would have been expected. Silver at mass 109 was measured. A theoretical plasma species, that could interfere, is the trimer $^{35}Cl(^{37}Cl)_2$, which also has a mass of 109. Experience has shown that this trimer is not normally abundant in the plasma so its interference is negligible (I. Finch, pers. comm.). If it had been present, its effect would have been detected and removed by the reagent blank. Large amounts of Cd and Pd would have had to have been

present for their scarce 108 isotopes to form interfering hydrides at mass 109, but this is not so. The only remaining mass 109 interference is the hydroxide $^{92}Zr^{16}O^{1}H$ (T.K. Chan, pers. comm.). Zirconium would not have been present in the reagent blank but, though it is present in the samples, there is no significant correlation of Ag with Zr, as would be expected, had Zr been a source of interference. Thus it is difficult to discount the ICP/MS Ag data from an analytical viewpoint.

The geochemical data for the complete soil and each of three soil fractions, comprising 9 major and 30 trace elements, are tabulated in Appendix 1, displayed graphically in Appendix 2 and are shown as frequency distribution plots in Appendices 3-6. A data disc is supplied as Appendix 10.

Except for data from the ICP/MS, all data below the detection limits have been reported without censorship, to aid future mathematical treatment. It must be emphasised that values in this range are of suspect precision, are estimates and should be interpreted with caution. Reference should be made to Table 3 for the detection limits.

4.6 Sequencing and Standards

The samples were analysed in random order and in-house weathered rock standards (STD 8 and STD 9) were introduced into the analytical batches at a ratio of 1:10 to 1:15, to monitor both accuracy and precision. The performance of the analytical method in relation to these standards, together with their mean values, standard deviations and the currently accepted values for these standards are reported in Appendix 1. The results are generally satisfactory in terms of both accuracy and precision. The results for the standards for the low-level elements Ag, Bi, Cd, In, and Sn, now being determined by ICP/MS rather than by XRF, from which the preferred values were taken, reflect our improved knowledge of them, rather than poor data.

4.7 Petrography

Ultrasonically cleaned samples of all size fractions, except the clays and $<75\,\mu$m fraction, were obtained and each examined under the binocular microscope. Thin and polished sections were prepared for petrographic examination. The polished sections were examined using both normally reflected light and oblique illumination from a fibre-optic source.

5.0 SOIL COMPOSITION

First the results of the pilot size fraction analysis are described and then the compositions of these fractions are investigated. This gave an insight into the origin of the soil components and helped in the design of the sample preparation method to be used on all soil samples.

5.1 Pilot Size Fraction Analysis

Four samples were selected for an orientation study from line 38820N: BC401, BC408, BC411 and BC418. Two were collected close to ore (BC408 and BC411) and the others relatively distant from ore, so as to be as representative as possible of the whole suite.

Small subsamples were split off each main sample for size fraction analysis. Six size fractions from each subsample at 2000-710, 710-500, 500-250, 250-142, 142-75 and $<75\,\mu$m were separated by sieving. Details of the method are given in Section 4.2. The $<2\,\mu$m fraction was partly extracted from the $<75\,\mu$m fraction by sedimentation in water. Each fraction was weighed. The percentage yields are presented in Table 4 and are shown graphically in Figure 4A.

TABLE 4
SOIL ORIENTATION
SIZE FRACTION ANALYSIS

	BC401 Wt %	BC408 Wt %	BC411 Wt %	BC418 Wt %
2000-710 μm	31.3	31.2	23.8	30.3
710-500 μm	16.6	15.4	13.2	14.6
500-250 μm	16.3	14.9	16.8	18.0
250-142 μm	15.5	15.9	21.1	15.7
142-75 μm	13.5	14.1	16.8	13.0
75-2 μm	5.1	7.0	6.9	6.4
<2 μm	1.8	1.5	1.3	1.8

The dominant fraction is the coarse 710-2000 μm ferruginous size fraction. One to three sand size fractions, centred around 250 μm, form a secondary mode. A binocular microscopic study of all size fractions indicated that iron-rich fragments were concentrated in the coarse and, to a lesser extent in the the finest fractions, the intermediate fractions being relatively sandy.

5.2 Compositions of Size Fractions

The external features of the various size fractions of sample BC401 were further examined using a binocular microscope and internal features were studied in both thin and polished section.

2000-710 μm
This size fraction consists of about equal proportions of quartz grains and black to brown goethitic granules (Figure 5A). All ferruginous granules show a high degree of sphericity and most are subrounded to rounded, though a few are subangular to angular. Most of the quartz grains consist of several crystals, with polygonal to sutured internal grain margins. The crystals show varying amounts of strain, indicating a vein quartz origin. There are also a few lithorelic grains, variably stained and cemented by goethite, and some unweathered grains of microcline. All quartz grains are thinly coated by goethite, which has penetrated into the interiors of some grains along crystal margins. The ferruginous, granular material shows dominant, bright, massive to spongy, secondary goethite fabrics, with some dehydration features. Other granules are rich in ferruginous clay. None have cutans, though the margins of some are slightly brighter than their interiors. This material is described in detail below.

710-500 μm
Quartz granules dominate the ferruginous granules (in the ratio of 65 to 35). A small, though significant, proportion of unweathered, slightly cleaved microcline (Figure 5B) occurs among the transparent grains, together with dominant vein quartz and a few clay-rich lithorelic grains. All the grains have a thin goethite coating. Secondary goethite structures dominate the ferruginous granules. Some are composite and contain clay-rich pisoliths, set in colloform goethite.

500-250 μm
Quartz is even more dominant over the ferruginous granules (85 to 15) than in the 710-500 μm fraction. The quartz grains are more rounded. There is a similar proportion of single crystal quartz grains to composite quartz grains to grains of microcline and saprolite. All have a thin goethite coating (Figure 5C). The opaque granules consist of ferruginous clay and rounded fragments of bright, secondary goethite.

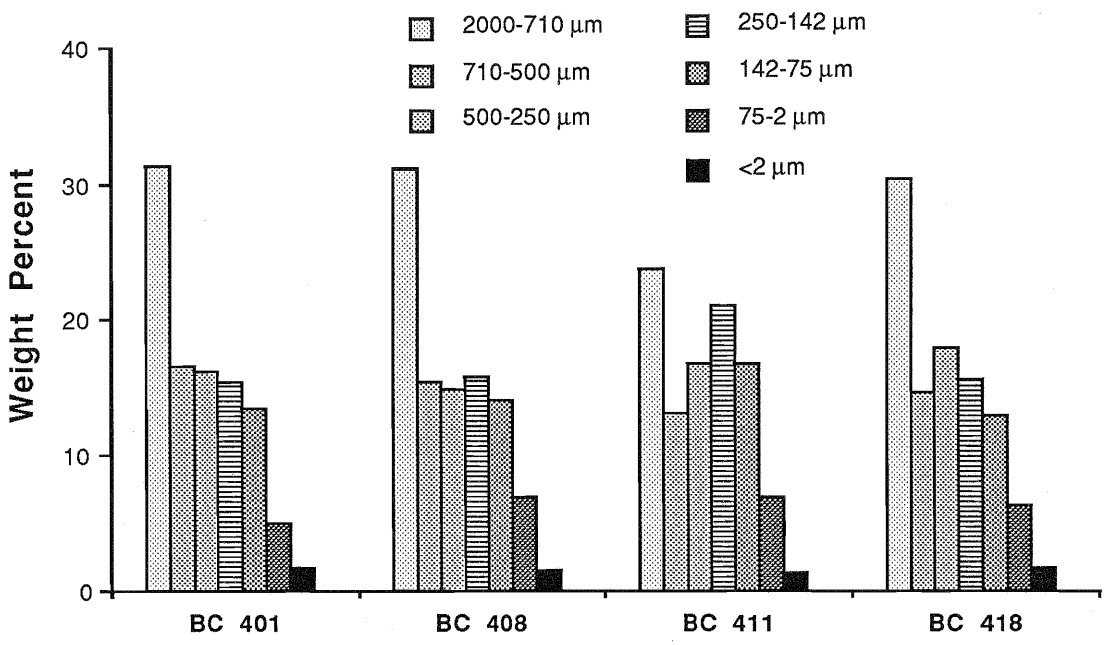

Figure 4A. Size fraction analysis.

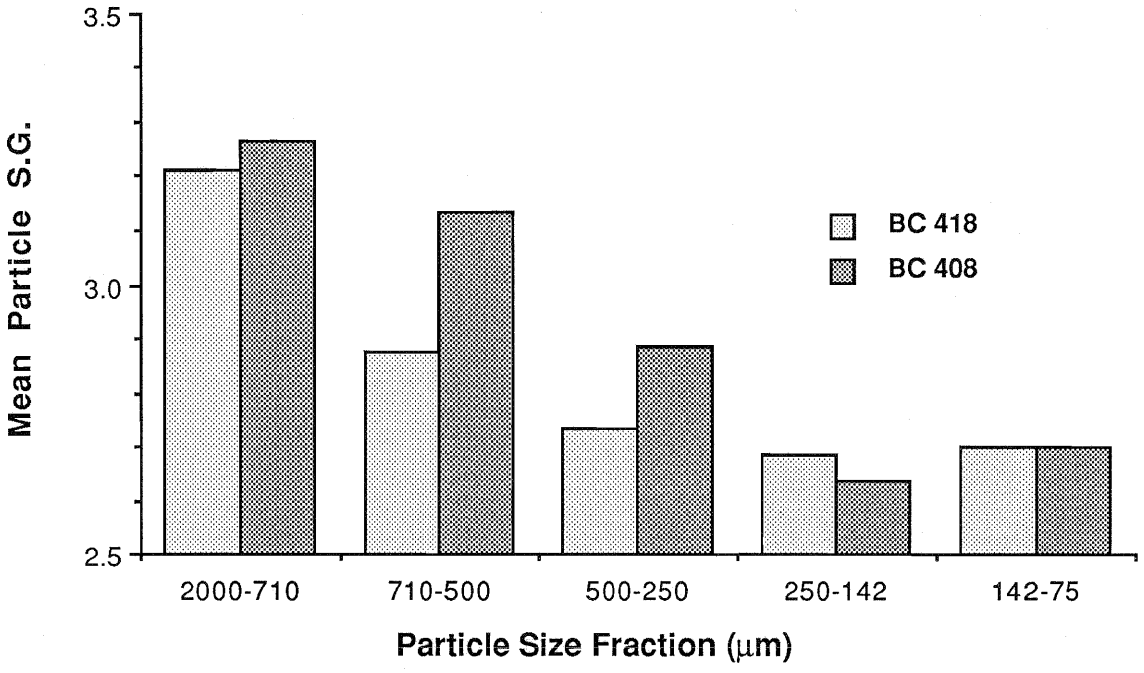

Figure 4B. Mean particle densities for size fractions.

250-142 μm
Quartz is dominant (Figure 5D) over the ferruginous granules (95 to 5). The grains are well-rounded and have well-developed, red goethite coatings. Round, unweathered microcline grains are more abundant than in the coarser fractions. The opaque granules consist of ferruginous clay and rounded fragments of bright secondary goethite.

142-75 μm
Though quartz is still dominant, the proportion of ferruginous granules has increased slightly (90 to 10). The quartz grains are rounded to subangular with little variety.

The increased proportion of quartz sand to goethitic granules in the middle and smaller fractions is illustrated by a decrease in the mean particle density (measured by pycnometer) of the fractions (Figure 4B). The high sphericity and roundness of the grains, together with their bright surfaces, suggests significant aeolian transport of the $<710\ \mu m$ material. Angular grains of vein quartz, presumed to be locally derived, form a very minor proportion of the sandy soil component. The presence of small quantities of unweathered microcline, having classic tartan twinning and perthitic structures (Figure 5B), indicates a granitic source for at least some of this wind-blown material.

Introduced aeolian quartz sand would act as a diluent, so the geochemically most useful fraction would seem to be the ferruginous $>710\ \mu m$ fraction. The potential of the commonly used $<75\ \mu m$ fraction, which appears to be slightly poorer in quartz and slightly richer in iron minerals and clay than the intermediate fraction, is unknown and needs to be assessed, as does the very small, but significant, clay-rich ($<4\ \mu m$) fraction.

6.0 PETROGRAPHY OF COARSE FERRUGINOUS COMPONENT

The petrographic information, that can be readily obtained from these ferruginous granules, is very limited because many of the overall petrographic relations are on a scale larger than that of the granule. A similar, and far clearer, history has been obtained from the coarse lag (Robertson, 1989).

The ferruginous granules of the soil are similar to the fine lag, into which they have been shed by deflation of the upper soil layers. The petrography and morphology of these soil granules is summarised briefly below for four samples from line 38820N. These are BC401 and BC418, from the flat ground on either side of the hill at 33600 and 34250E respectively and represent geochemical background. In contrast, samples BC408 and BC411 are from the immediate footwall and hangingwall of the orebody at 33925E and 34000E respectively. They consists of black, nodular, goethitic granules, some of which are magnetic, red to yellow ferruginous, clay-rich granules, quartz fragments and rare, cellular ironstone. There are also granules of calcrete and aggregates of sand with a calcareous or siliceous cement (hardpan). The proportions of cellular ironstone fragments are significantly greater in BC408 and BC411, which lie close to the orebody. Each sample was manually split into four components, namely red, ferruginous clay (Figure 5E), yellow clay (Figure 5F) and a black, magnetic (Figure 5G) and a black, non-magnetic (Figure 5H), goethitic component. Each was mounted separately for polishing.

The petrography indicates a similar range of fabrics to those encountered in the fine and the coarse lag (compare Figures 5E-H with the frontispiece in Robertson, 1989). These include lithorelics, containing remnant muscovite (Figure 6G) and goethite pseudomorphs after saprolitic kaolinite (Figure 6H). Some pseudomorphs after kaolinite have vermicular, authigenic, accordion structures (Figure 6A), that developed in the saprolite during weathering and have been completely replaced by goethite. These pseudomorphs are set in secondary goethite, which varies considerably in reflectivity, due to variable and

FIGURE 5
SOIL COMPONENTS

A. The 710-2000 μm fraction contains a large proportion of black to very dark brown, shiny, ferruginous soil granules (GO), rich in goethite, and dark, red-brown to yellow granules of ferruginous clay (FC), with a slightly lesser proportion of white and red-brown quartz (QZ). All show a high degree of sphericity and most are sub-rounded to rounded. Close-up photograph.

B. The 500-710 μm fraction. A grain of unweathered microcline (MC), showing tartan twinning and a perthitic structure, together with slightly-strained, vein quartz (QZ). Photomicrograph under crossed polarizers. Co-ordinates 33600E 38820N.

C. The 250-500 μm fraction. This consists of dominant quartz (QZ) and a few ferruginous granules (FG) and crystals of microcline showing cleavage (MC). All are well rounded and have thin coatings of goethite (CT). Photomicrograph in plane polarized light. Co-ordinates 34250E 38820N.

D. The 142-250 μm fraction. Quartz (QZ) dominates the ferruginous granules (FG), some of which are ferruginous clay (FC). All grains are well rounded and most are thinly coated with goethite. Close-up photograph.

E. Yellow-brown clay granules. The brown granules (HC) consist of kaolinite stained with hematite and the yellow granules (GC) are kaolinite stained with goethite. One hematitic clay granule has a partial rind of goethitic clay (RZ). Many granules are cut by vermiform channelways, lined with dark goethite (CA) and some contain patches of goethitic and hematitic clays. Close-up photograph. Co-ordinates 33925E 33820N.

F. Yellow clay granules. The yellow granules (GC) consist of kaolinite stained with goethite. Some are massive (MC), others vesicular (VC) and even cavernous. Some contain mixtures of goethitic and hematitic clays (MX), others are cut by channelways (CH), lined with hematitic clay. Close-up photograph. Co-ordinates 33600E 38820N.

The clay-rich granules, illustrated in E and F, are all well rounded. They are not distinct species but grade into one another and some granules are mixtures of both types.

G. Black magnetic granules. These are generally more angular than the clay granules. Some are lithorelics (LR), with obvious foliated structures, but, in others, the foliation is less apparent. Many consist of massive goethite (MG) or have colloform structures. Some are fragments of granules (FG) and have cutans of massive goethite and attached, hardpan-related, siliceous or clay coatings (SC). Close-up photograph. Co-ordinates 33925E 38820N.

H. Black, non-magnetic granules. Most consist of massive, secondary goethite (GO) with inclusions of quartz. Many show several goethite phases with fabrics indicating multiple deposition of iron oxides (MF). One fragment is of a gossan (GN), showing a boxwork, indicative of weathered sulphides. Close-up photograph. Co-ordinates 33925E 38820N.

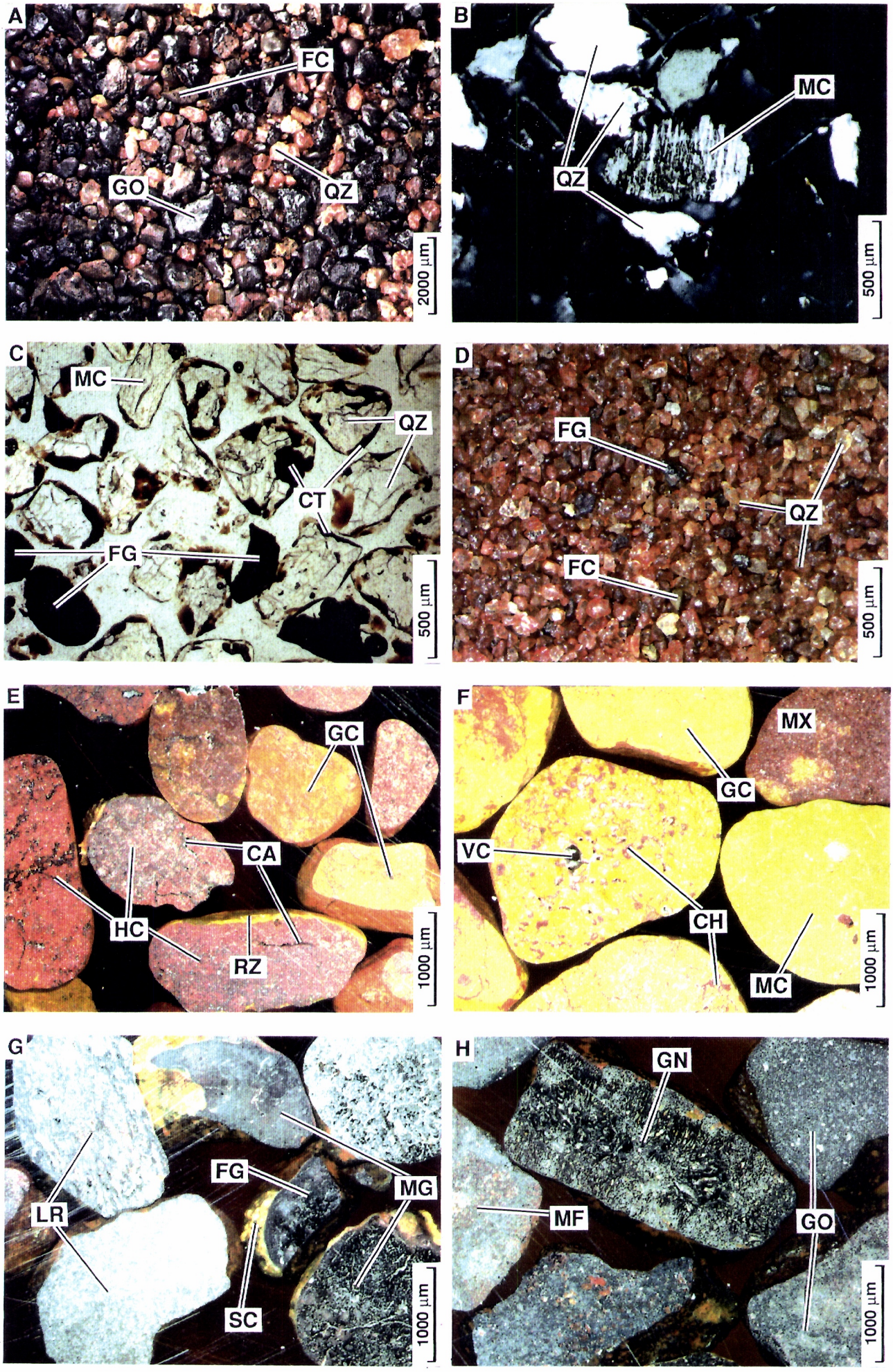
A
FC
GO
QZ
2000 µm
B
MC
QZ
500 µm
C
MC
QZ
CT
FG
500 µm
D
FG
QZ
FC
500 µm
E
GC
CA
HC
RZ
1000 µm
F
MX
GC
VC
CH
MC
1000 µm
G
FG
MG
LR
SC
1000 µm
H
GN
MF
GO
1000 µm

FIGURE 6
PETROGRAPHY OF FERRUGINOUS GRANULES

A. Ferruginous soil granule consisting of spongy, secondary goethite (G), pocked with vesicles (V) and containing several 'accordion' structures (A) which pseudomorph previous saprolitic 'authigenic' kaolinite. Specimen BC401. Co-ordinates 33600E 38820N.

B. A complex ferruginous soil granule which contains pisoliths of ferruginous clay (FC), coated with cutans of low reflective goethite (G), set in highly reflective, partly dehydrated goethite (QH). Specimen BC401. Co-ordinates 33600E 38820N.

C. Ferruginous soil granule, showing an early, partly dehydrated, strongly reflective goethite (GA), with dehydration cracks. These cracks have been filled with a later, less reflective, slightly spongy goethite (GB). The granule is partly coated with a ferruginous clay cutan (CL). Specimen BC408. Co-ordinates 33925E 33820N.

D. Cinder-like, ferruginous gossan soil granule, showing structures suggesting previous pyrrhotite or marcasite and possibly some chalcopyrite or galena. Specimen BC408. Co-ordinates 33925E 33820N.

E. Part of a brown granule, consisting of ferruginous clay (FC), pocked by vesicles (V), linked by solution channels (SC) which have subsequently been filled with goethite (G). Specimen BC408. Co-ordinates 33925E 33820N.

F. Goethitic pisoliths (P), with well-developed, concentric fabrics, set in spongy, secondary goethite (G), pocked with vesicles (V). Magnetic goethitic soil granule. Specimen BC411. Co-ordinates 34000E 38820N.

G. Magnetic, ferruginous soil granule showing relict micas (M), set in spongy, secondary goethite (G). The mica sheets are exploded and goethite has penetrated between them. Fabrics of this type are associated with the phyllitic ore host, so significant down-hill transport of this granule may be inferred. Specimen BC418. Co-ordinates 34250E 33820N.

H. A sworled fabric of pseudomorphed saprolitic kaolinite (PK), set in bright goethite (G) in a ferruginous, magnetic soil granule. Specimen BC418. Co-ordinates 34250E 33820N.

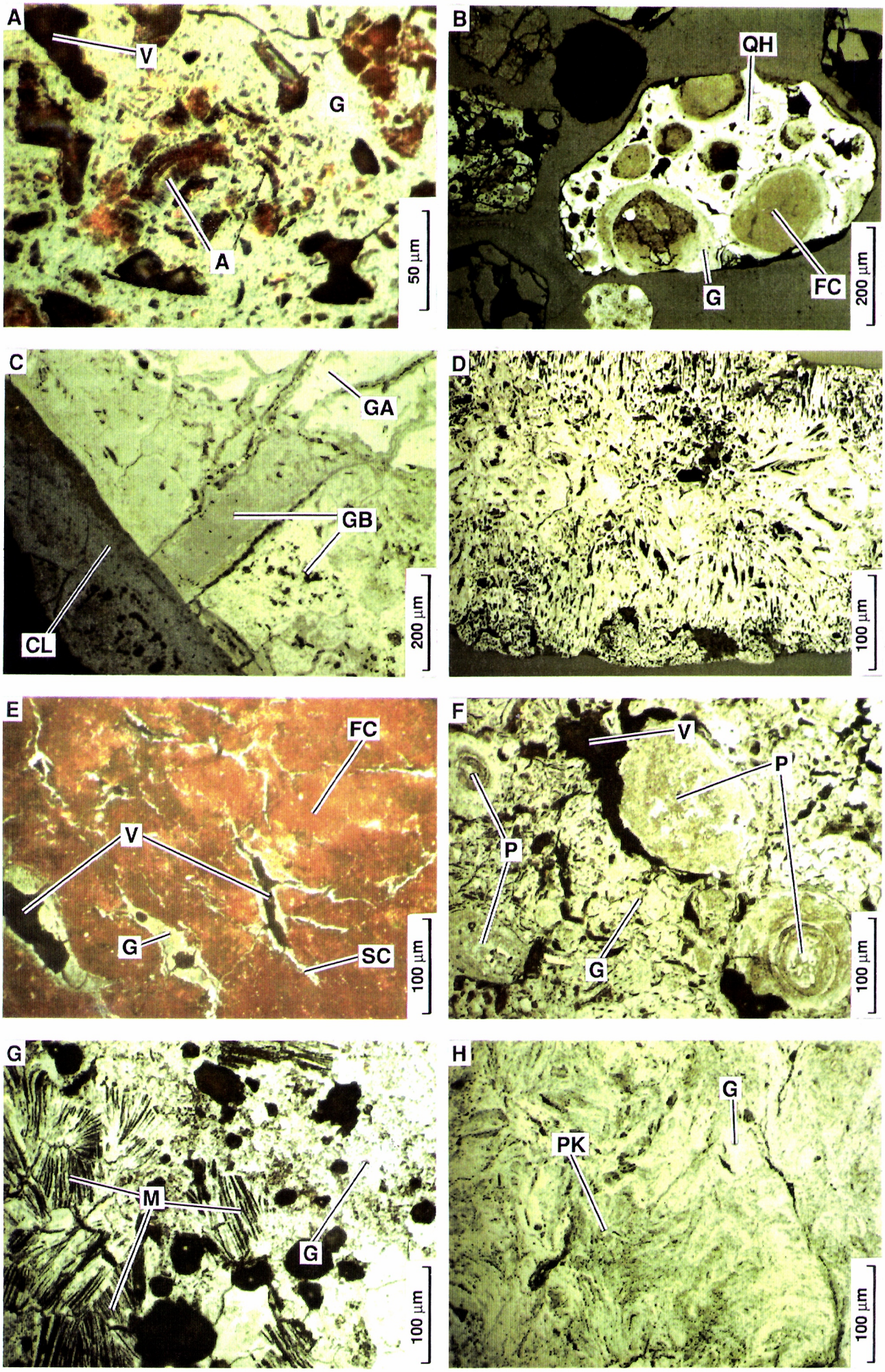
A
V
G
A
50 µm
B
QH
G
FC
200 µm
C
GA
GB
CL
200 µm
D
100 µm
E
FC
V
G
SC
100 µm
F
V
P
P
G
100 µm
G
M
G
100 µm
H
G
PK
100 µm

partial dehydration to hematite (Figure 6C). The goethite may be massive, spongy, vesicular (Figure 6F) or colloform, with some dehydration cracks. The red and yellow clay fragments consist of kaolinite mixed with minor but variable amounts of goethite. Several clay generations are apparent with early clay fragments enclosed in a more or less ferruginous clay. Some clay fragments contain earlier goethite-rich lithorelics, complete with mica remnants and layer silicate pseudomorphs. Some fractures, vesicles and solution channels in the clay are lined or sealed with grey goethite (Figure 6E; see also Robertson, 1989, Figure 9H). The cellular ironstone consists of fragments of gossan, with fabrics (Figure 6D) possibly derived from primary pyrrhotite or marcasite, chalcopyrite and galena.

Detailed petrographic descriptions of individual samples follow.

BC401

The magnetic goethitic fragments largely show secondary goethite structures, including dehydration cracks filled with grey goethite, vesicles lined with a thin goethite layer, massive, spongy goethite and colloform structures. Layer silicate pseudomorphs are very fine grained and are relatively rare. They consist of indistinct, very small booklets, set in spongy goethite, rich in irregular shaped vesicles.

The non-magnetic fragments show similar structures, with a few layer silicate pseudomorphs, including delicate accordion structures after kaolinite (Figure 6A). Secondary structures include fragments of early, spongy, secondary goethite, enclosed in even later goethite, dehydration cracks and small lozenge-like crystals of hematite.

The red clay granules contain a few fragments of early ferruginous clay, enclosed in a later, even more ferruginous clay (Figure 6B). Fractures and solution channels in some clay granules have been lined with grey goethite. The yellow clay fragments show similar features but a wider variety.

BC408

The magnetic fraction consists of a variety of goethite-rich fragments, some of which contain a few remnants of pseudomorphed layer silicates, set in banded and massive secondary goethite. The pseudomorphs of layer silicate consist of expanded book structures and rare accordion structures; most were probably derived from kaolinite but a few are interleaved kaolinite and muscovite. There are several generations of secondary goethite, some with dehydration cracks (Figure 6C) and others with fragments of earlier phases embedded in later phases. Some granules have narrow, partial cutans of laminated goethite, generally with a bright, outer rim. Some of the secondary goethite-rich fragments are rich in vesicles.

The non-magnetic fraction has a higher proportion of secondary goethite than the magnetic fraction. Layer silicate structures are rare. One fragment has a cinder-like appearance and appears to be a gossan. It contains goethite structures (Figure 6D) possibly after pyrrhotite or marcasite with some possible chalcopyrite or galena (E.H. Nickel - pers. comm.). This sample site is close to the orebody subcrop. The brown granules consist largely of several generations of ferruginous clay (kaolinite with minor goethite), some of which are included as fragments in a younger, ferruginous clay matrix. Solution channels in the clay fragments are lined or filled with late goethite (Figure 6E).

BC411

The magnetic fragments are dominated by secondary goethite structures, although a few, fine-grained, generally indistinct, goethite pseudomorphs after kaolinite remain. The non-magnetic fraction has a higher proportion of layer silicate pseudomorphs which vary considerably in both size and fabric from one grain to another. Secondary structures include fibrous, colloform goethite, and concentric, pisolitic structures (Figure 6F).

The red clay granules, which enclose some very ferruginous fragments, have a variety of fabrics, including breccias and goethite infillings of vesicles and solution channels. The yellow clay fragments are similar but more spongy and vesicular.

BC418
The magnetic fraction is unusually rich in layer silicate relicts and pseudomorphs. The relicts are mica (Figure 6G) and the pseudomorphs probably after kaolinite (Figure 6H). The non-magnetic fraction generally contains goethite of lower reflectance and there are fewer layer silicate pseudomorphs. The pseudomorphs have expanded book structures and are probably after kaolinite. Secondary structures, including spongy and massive types, predominate. Some grains have a highly reflective rim of goethite.

The red clay fragments consist of a spongy ferruginous clay (kaolinite with minor goethite), containing irregular vesicles as well as patches and lozenges of hematite. Some of the smaller vesicles are lined with goethite, which also fills channels linking the vesicles. A second generation of larger vesicles are unlined and cut the solution channel fabric. The yellow, clay-rich fragments show a wide variety of fabrics from internally brecciated, vesicular to externally pisolitic. A few pieces of earlier, bright goethite, containing mica relics and layer silicate pseudomorphs, are incorporated in the clay granules.

7.0 MINERALOGY

All complete soil samples and all samples of the $<4\,\mu$m fraction samples were examined by XRD at Floreat Park (this is referred to as the 'large data set'). A small number of samples were selected for a detailed XRD study on a more modern diffractometer at North Ryde. These were selected so as to represent, as far as possible, the extreme east and west ends of the soil sampling traverses, as well as locations close to the ore position and 'regional' background ('small data set'). All four fractions were examined so that their mineralogy may be compared and the effects of fractionation may be assessed.

Overall, the mineralogy of the soil was found to be relatively simple, being a mixture of quartz, kaolinite and the iron oxides, hematite and goethite, with minor sericite.

7.1 Limitations

In the large data set, semiquantitative estimates of the contents of quartz, kaolinite and sericite were made by measurement of the diffraction peak heights (see Section 4.4 and Table 2). Iron oxides are also present as major components; however semiquantitative estimation of goethite and hematite was not possible due to considerable peak overlap with kaolinite, quartz and sericite.

In the smaller data set, the extra sensitivity allowed additional semi-quantitative estimation of calcite and feldspar. For similar reasons, goethite and hematite could be determined only qualitatively.

7.2 Results

First the effect that fractionation of the soil has had on the mineralogy is assessed. Variations in those major minerals that could be determined semi-quantitatively along the soil sampling lines for the complete soil and the $<4\,\mu$m fraction is presented and related to underlying lithologies.

Soil Fractionation
The mineralogical effect of soil fractionation is demonstrated using the small data set (Appendix 8) and this is illustrated in Figure 7. The complete soil consists of quartz and hematite, with some goethite and kaolinite, as well as minor rutile, calcite, feldspar and sericite in some. The 710-4000 μm fraction

FIGURE 7

The mineralogical effect of soil fractionation on the contents of quartz, kaolinite, sericite, calcite and feldspar

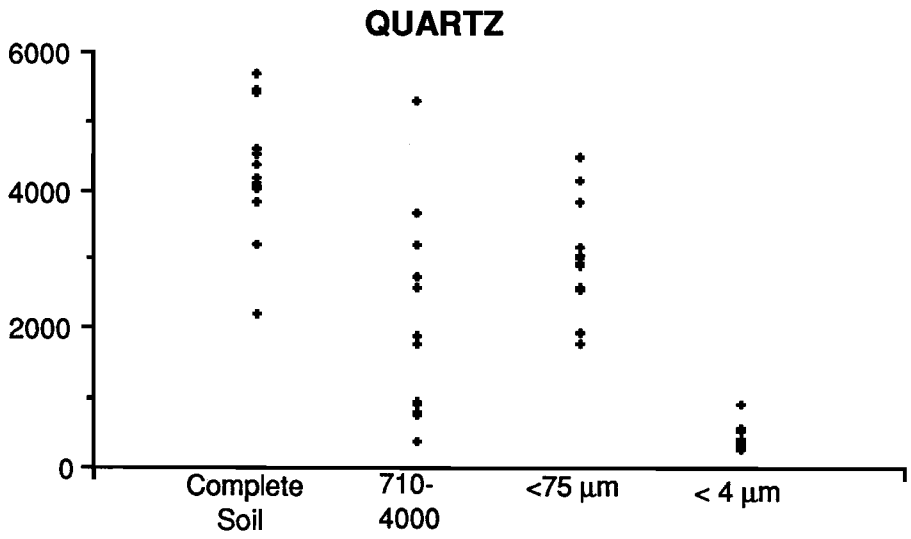
QUARTZ
6000
4000
2000
0
Complete Soil
710-4000
<75 µm
< 4 µm

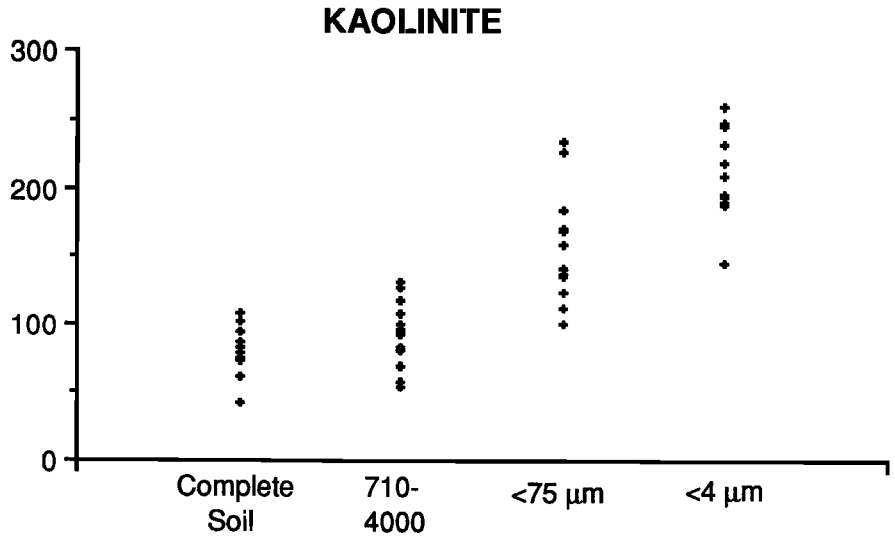
KAOLINITE
300
200
100
0
Complete Soil
710-4000
<75 µm
<4 µm

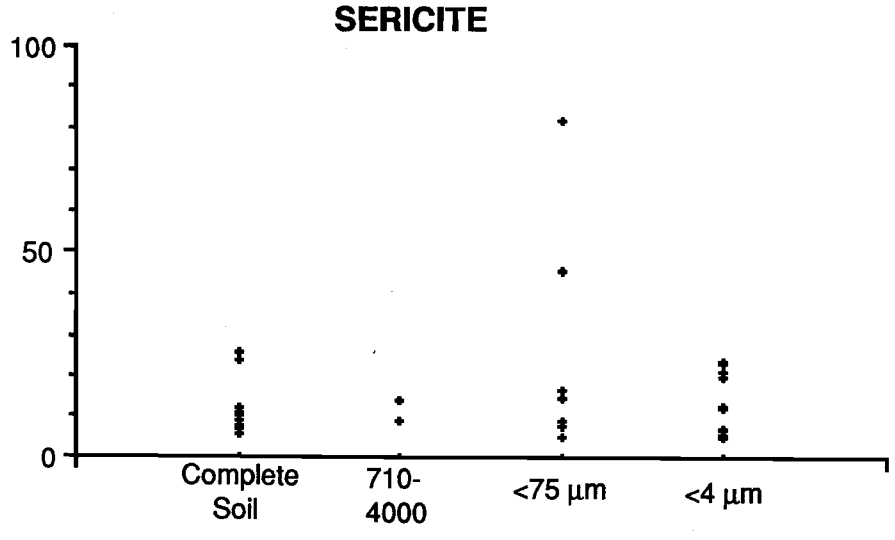
SERICITE
100
50
0
Complete Soil
710-4000
<75 µm
<4 µm

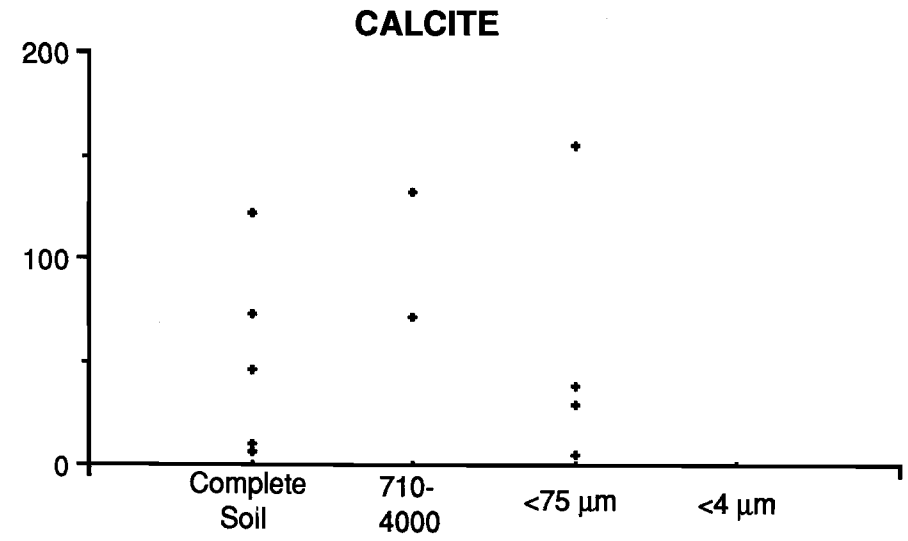
CALCITE
200
100
0
Complete Soil
710-4000
<75 µm
<4 µm

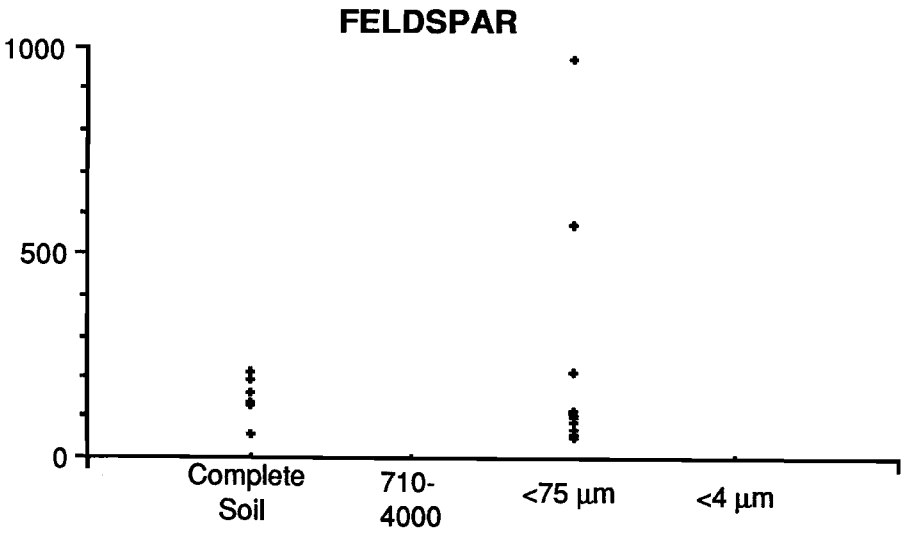
FELDSPAR
1000
500
0
Complete Soil
710-4000
<75 µm
<4 µm

FIGURE 8

Smoothed mineralogical traverses along lines 38820 and 38940N for quartz, kaolinite, sericite in the complete soil and the <4 μm fraction.

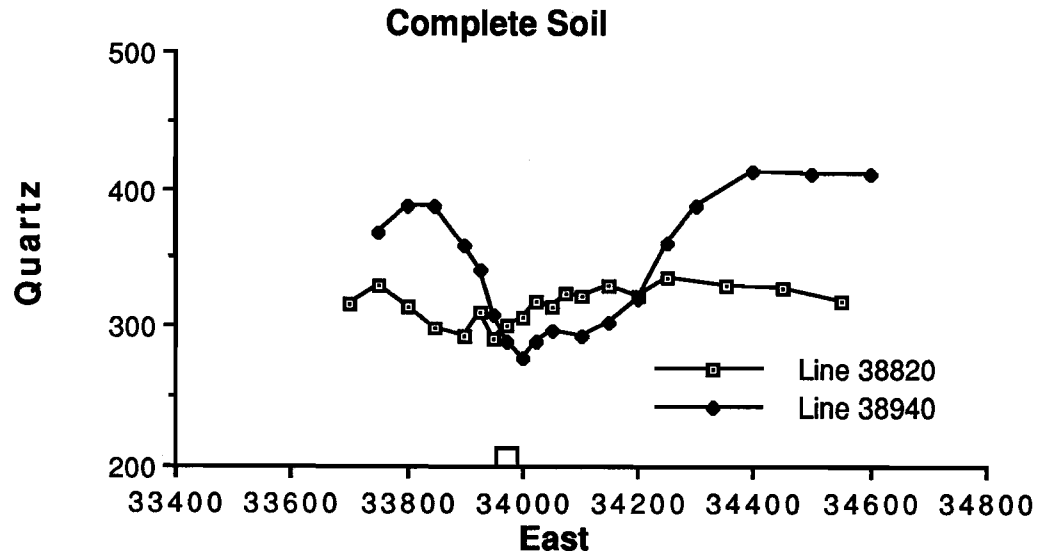
Complete Soil
Quartz
500
400
300
200
Line 38820
Line 38940
33400 33600 33800 34000 34200 34400 34600 34800
East

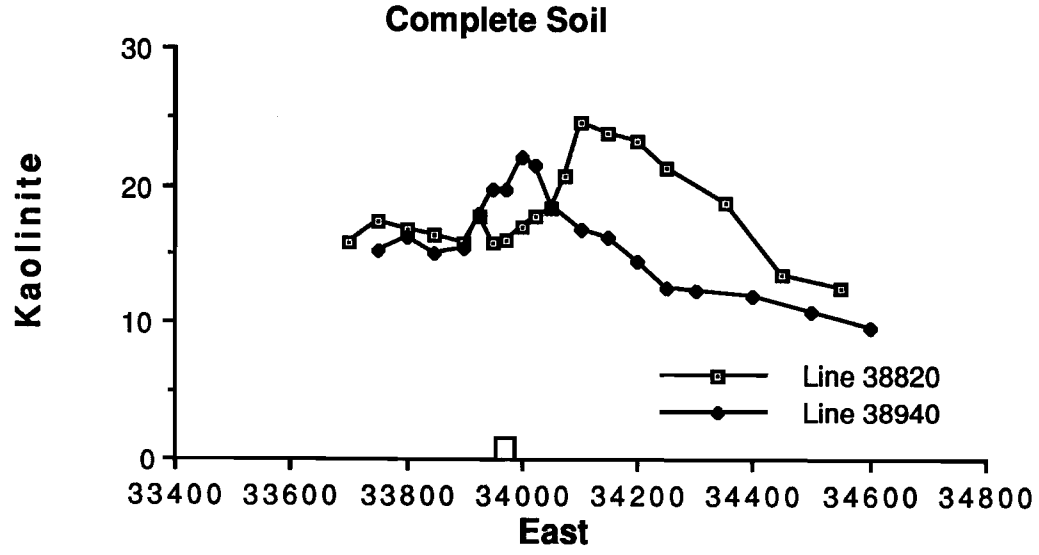
Complete Soil
Kaolinite
30
20
10
0
Line 38820
Line 38940
33400 33600 33800 34000 34200 34400 34600 34800
East

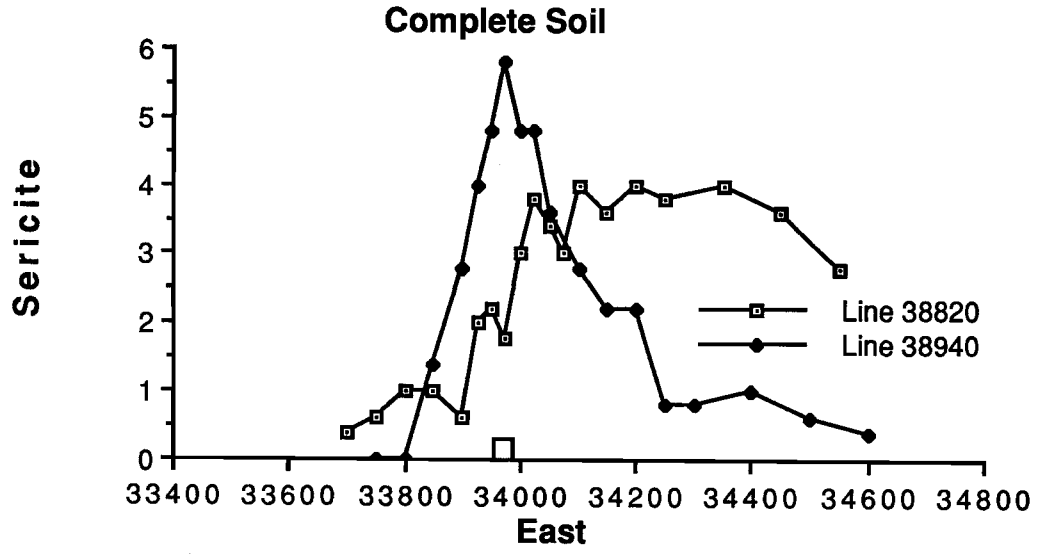
Complete Soil
Sericite
6
5
4
3
2
1
0
Line 38820
Line 38940
33400 33600 33800 34000 34200 34400 34600 34800
East

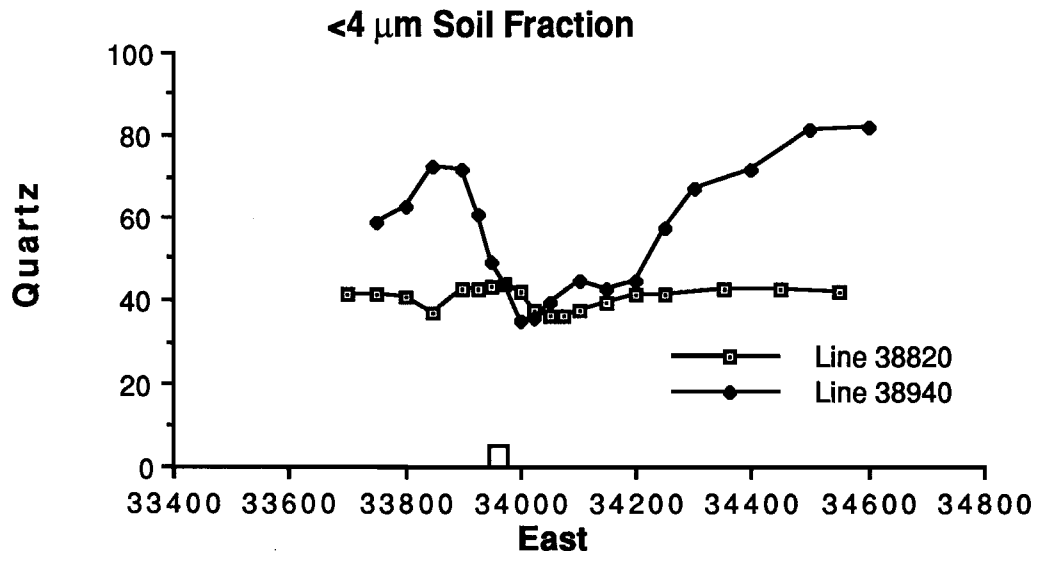
<4 μm Soil Fraction
Quartz
100
80
60
40
20
0
33400 33600 33800 34000 34200 34400 34600 34800
East
Line 38820
Line 38940

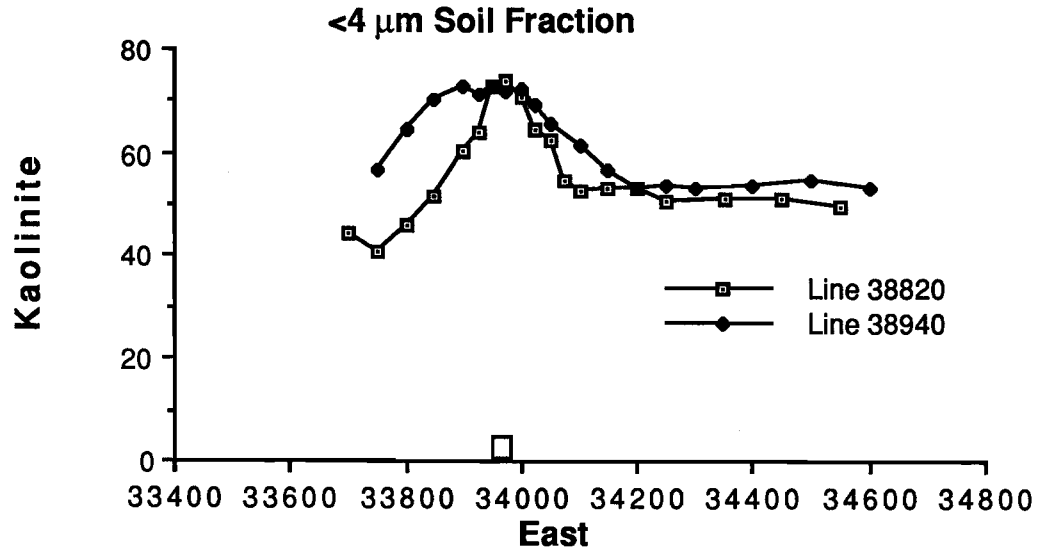
<4 μm Soil Fraction
Kaolinite
80
60
40
20
0
33400 33600 33800 34000 34200 34400 34600 34800
East
Line 38820
Line 38940

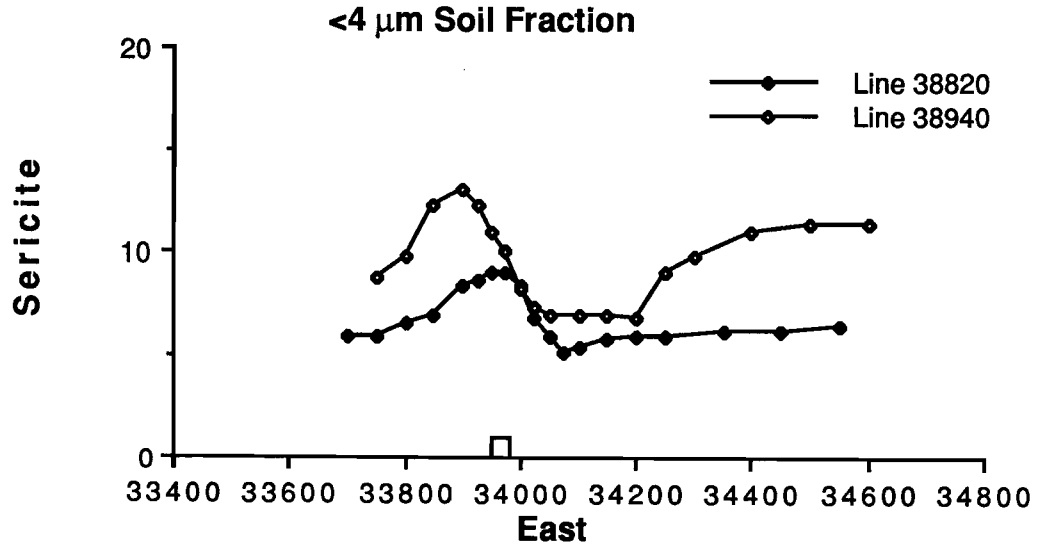
<4 μm Soil Fraction
Sericite
20
10
0
33400 33600 33800 34000 34200 34400 34600 34800
East
Line 38820
Line 38940

contains greater, but undetermined, quantities of hematite, goethite and kaolinite but significantly less quartz. It also contains minor calcite and rutile. The finer fractions contain progressively less quartz and more kaolinite. The abundance of sericite is similar in all soil components, although it has the widest range of abundance in the $<75\,\mu$m fraction, which consists of quartz, kaolinite, hematite and feldspar, with minor sericite, goethite and sporadic calcite. Persistence of feldspar in this fraction shows this fraction has been diluted by aeolian material. Feldspar has already been shown to be a significant component of the adjacent 75-710 μm fraction.

The $<4\,\mu$m fraction has the simplest mineralogy, containing only kaolinite, quartz, hematite and sericite with minor goethite. Feldspar and rutile were probably eliminated during sedimentation and most calcite would have been dissolved during acid flocculation of the clays (see Section 4.3). Small quantities of carbonate minerals may still remain, for Ca, Mg and Sr are present in the $<4\,\mu$m fraction, but the content is too low for detection by XRD. Sedimentation of the clays has also greatly reduced the abundance of quartz and goethite, whereas the concentrations of kaolinite, sericite and hematite have been enhanced.

Mineralogical Traverses
The mineralogy of the complete soil and the $<4\,\mu$m fraction along each traverse (larger data set) is shown in Figure 8. The semiquantitative data are, by their nature, noisy, so a five-point moving average has been used to smooth the data for plotting. The raw data are given in Appendix 9.

In both fractions there is a decrease in quartz over the lateritic duricrust and the ore position on line 38940N only and the quartz content is slightly elevated on the flat ground to the east of the ore body on line 38940N. Both fractions show an increase in the kaolinite content on both sample lines. This is centred on the ore position in the $<4\,\mu$m fraction and on line 38940N for the complete soil. In the complete soil, there is an increase in sericite abundance over the ore on line 38940N but, on line 38820N, sericite is abundant to the east of the ore position and into background. The $<4\,\mu$m fraction has a sericite maximum centred on the ore position on line 38820N but displaced slightly to the west on line 38940N. The small data set shows that calcite occurs in the soil near the top of the hill, associated with known outcrops of calcrete (Robertson and Churchward, 1989) and strong enrichments of Ca, Mg and Sr are present in the lag (Robertson, 1989) and in the soil (see Section 8).

Though the data need smoothing before plotting, the mineralogy of the soil, particularly the $<4\,\mu$m fraction, yields some useful lithological information. This appears to be due to the micaceous and kaolinitic nature of the saprolite of the ore host, which contrasts with the contiguous mafic and ultramafic rocks. This strongly suggests that $<4\,\mu$m fraction is dominantly local rather than aeolian in origin.

8.0 GEOCHEMISTRY

The geochemistry of the complete soil, and its constituent size fractions, are first discussed generally and then systematically, by elements, so that the performance of each size fraction can be compared and the signal produced by the centrally located sample line (38820N) can be compared to that located across the north end of the orebody (38940N). While reading the systematic geochemistry, reference should be made to the graphs in Appendix 2.

8.1 Geochemical Background

Establishing geochemical background is of crucial importance for evaluating orientation surveys. For this purpose a small database of four samples, remote from ore (Figure 1C), is herein referred to as 'regional' background. In addition, some of the samples from the eastern end of the soil survey lines may be in

'local' background (>34400E). The range of the 'regional' background data, together with their geometric mean, are given in Appendix 1; they are also plotted with the data from the soil survey lines (Appendix 2), so that the 'regional' and 'local' backgrounds may be compared with the element abundances near the ore. This comparison between 'local' and 'regional' background will reveal any anomalies or elevated backgrounds which exceed the size of the soil sample lines.

The 'regional' and 'local' background samples are underlain by a variety of weathered lithologies, including mafic and ultramafic Archaean rocks and Permian tillites. In consequence some lithological variation in background is to be expected. Nevertheless, they are all 'distant' from ore and their background levels are generally consistent and realistic in practice.

8.2 Inter-element Correlations

Inter-element correlations have been investigated by means of correlation matrices (Appendix 7). For 45 samples, any correlation over 0.300 is statistically significant at the 95% confidence limit. In the following text, those correlations in the range 0.300-0.499 are classed as weak, those of 0.500-0.699 as moderate and those >0.700 as strong. Particular significance has been accorded to significant correlations which occurred in related fractions (e.g., <75 μm and <4 μm fractions, collectively called the 'fine' fractions) or in all the soil fractions. The influence of outliers on the correlations was investigated by examining XY plots of all those element pairs which showed a significant correlation (>0.300). The strengths of the correlations were notionally reduced if outliers appeared to have had an undue influence. This is reflected in the text but not in Appendix 7, which contains the raw statistical data. The inter-element correlations may be used to provide a hint as to the mineralogical siting of trace elements.

8.3 Major and Minor Oxides

Silicon is concentrated as quartz in the wind-blown sandy component of the complete soil and in the <75 μm fraction. Its abundance is least in the 710-4000 μm fraction where it shows a decrease over the ore host and the lateritic duricrust. This is matched by a corresponding increase in Fe abundance.

The relationships between the major oxides of Si, Al and Fe are shown in Figure 9 for the complete soil and its three size fractions. The 710-4000 μm fraction is the most Fe-rich but, although the Si:Fe ratios vary considerably, the Al content remains relatively constant. This spread of data is similar to the Si:Al:Fe relationship in the fine lag, where there is a tendency for the high Au samples to be comparatively Fe-rich (Robertson, 1989; Figure 12). In comparison, the <75 μm fraction has a relatively consistent Fe content and possibly a consistent Fe:Al ratio, but the Si content varies significantly. This probably reflects variation in the content of wind-blown sand and, at least in part, the efficiency of separation of the clay fraction. The Si:Al:Fe composition of the <4 μm fraction is the most consistant.

The mid-range alkaline earth elements Ca, Mg and Sr show sharp peaks related to a high soil pH and to calcrete outcrop and subcrop. These peaks lie close to the top of the hill and, fortuitously, to the subcrop of the ore host. A coincident peak in P is ascribed to bone fragments from animal burrows under the calcrete. Sulphur shows a maximum over the ore and it is correlated with Ba in the coarse soil fraction. Both barite and gypsum have been noted at Beasley Creek.

SiO_2

The complete soil and the <75 μm fraction are particularly siliceous, reflecting an appreciable wind-blown quartz content. In contrast, the 710-4000 μm fraction is Si-poor. It shows a decrease in silica over ore relative to 'local' and 'regional' background, similar to the distribution shown by the fine lag. This localised decrease in Si is reflected weakly in the complete soil. All other fractions show no Si minimum.

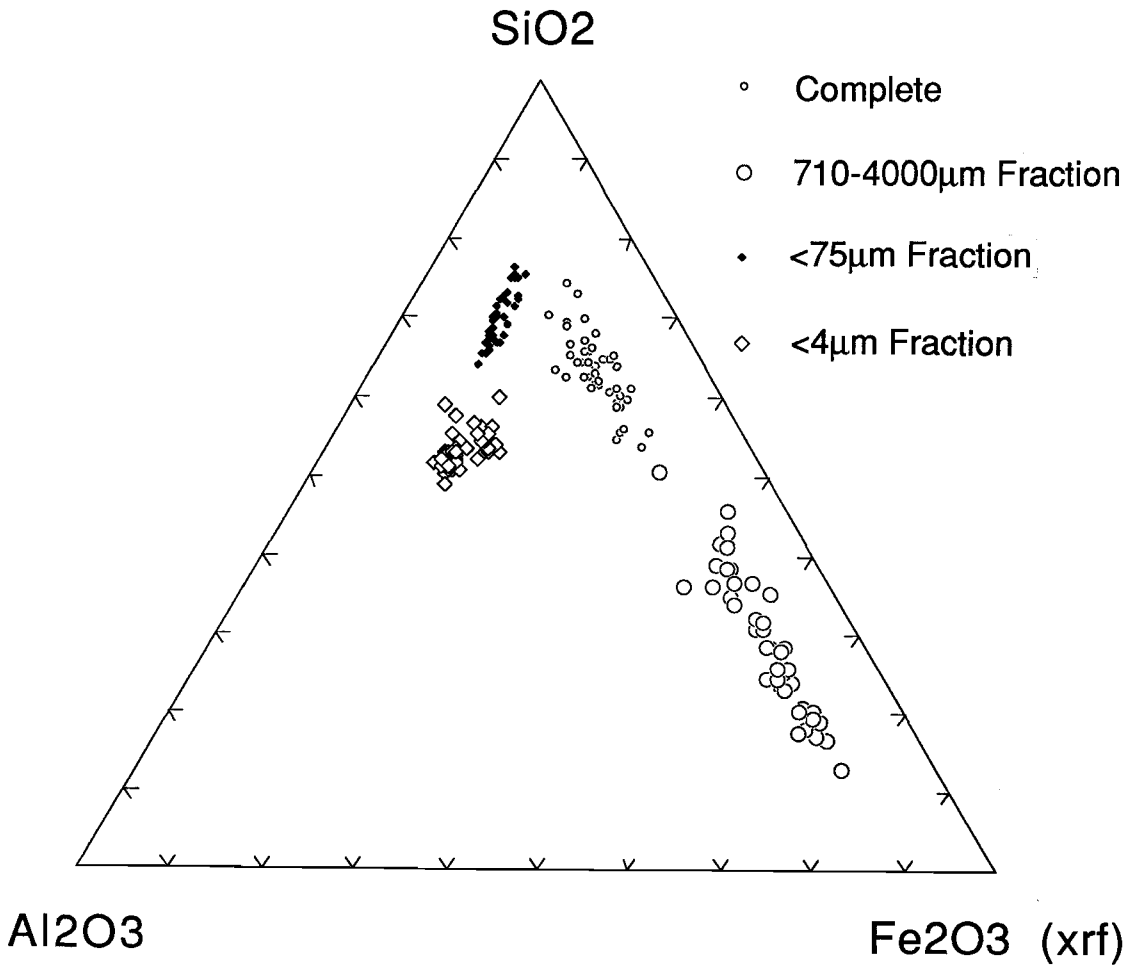

Figure 9. Ternary diagram of the major oxides of the soil components.

'Local' and 'regional' backgrounds are similar. Silicon is normally distributed in all soil fractions except for the 710-4000 μm fraction, where the distribution appears to be polymodal.

Al_2O_3

The Al content of the complete soil shows a weak increase and there is a slightly stronger increase in the <4 μm fraction over the lateritic duricrust. In contrast, samples overlying the ore zone are less abundant in Al. The Al abundance in 'regional' and 'local' background samples are very similar, though the variance in 'regional' background is small compared to that of the 'local' background. Aluminium is correlated strongly with Ga in all fractions, with Rb in the complete soil, with Ni and Rb in the <75 μm fraction and with La in the <4 μm fraction.

Fe_2O_3

The 710-4000 μm fraction is the most Fe-rich soil component and the Fe content of this fraction is greatest over the ore zone and the lateritic duricrust. This distribution is similar to that of the fine lag. The complete soil shows this also but iron is less abundant and the contrast is smaller. The Fe content is less by a factor of more than 4 in the <75 and <4 μm fractions. Iron is strongly correlated with V in all soil fractions and with Ti in most.

MgO and CaO

The major alkaline earth elements, Mg and Ca (as well as Sr - described separately) show similar distributions. Similar sharp and localised increases in Mg and Ca occur in most fractions on both sample lines, though the strengths of the peaks are greater on line 38940N, where they closely approximate the position of the ore. They tend to the footwall on line 38820N. Though the peaks are stronger in the soil than in the fine lag by a factor of 4-5, they lie in similar positions. The strongest Mg peaks and peak to background contrasts occur in the two fine fractions, the <4 μm fraction being slightly more Mg rich than the <75 μm fraction. Ca is not as strongly concentrated in the fine fractions as is Mg. These Mg and Ca peaks are coincident with similar Sr peaks and appear to be related to the occurrence of soil carbonate and calcrete outcrop (Figure 1D) rather than to mineralisation, as these three elements are strongly correlated with soil pH. Correlation of Mg and Ca with Sr is weakest in the <4 μm fraction.

Na_2O

There is a strong disparity between the data gathered from XRF and those provided by the ICP. The ICP data, which lies in the range 0.2-0.8% Na_2O is ignored for reasons presented in Section 4.5.

There is a small increase in Na concentration over the footwall rocks, principally in the complete soil and in the <75 μm fraction. The increase is much less apparent in the 710-4000 μm and the <4 μm fractions, in which the Na content is generally low. As the fine fractions were separated by wet sieving and clay sedimentation, it is unlikely that the contained Na is present as halite. It probably reflects minor Na-feldspar in the wind-blown sand component of the soil. This is supported by higher Na levels in the complete soil and in the <75 μm fraction, which are richer in sand. Sodium is weakly correlated with soil pH, Si and Sr.

TiO_2

Titanium does not seem to be preferentially concentrated in any particular soil fraction. Maximum contents are present over the lateritic duricrust in the 710-4000 μm fraction and in the fine lag. The two fine soil fractions have weak maxima in the footwall on line 38940N but the range in 'regional' background is very small. Titanium is correlated strongly with Nb and Zr in the fine fractions, and with Ga, V and W in the 710-4000 μm fraction. It probably largely occurs in the red-brown clay granules of the 710-4000 μm fraction (Robertson, 1989; Appendix 7), with clay in the <4 μm fraction and with heavy minerals in the <75 μm fraction.

P_2O_5

The ICP detection limit for P is 0.1% P_2O_5 and most of the data fall below this limit. The P contents in the background samples and both the sampled traverses are highest in the $<4\,\mu$m fraction. There is a strong single-point maximum in P on line 38940N, which rises significantly above the detection limit, and this is reflected at the same sample point in the complete soil and in the $<75\,\mu$m fraction, but not in the 710-4000 μm fraction. Despite the data lying mostly below the detection limit, the higher P background and the sharp P peaks are regarded as real. The peaks are reproducible between fractions and the high P background of the $<4\,\mu$m fraction persists despite randomisation of the samples of all fractions prior to analysis (Section 4.6). It is suspected that the P detection limit is overstated.

Apatite is readily soluble under acidic conditions. Released P could have been adsorbed by clay particles in the $<4\,\mu$m fraction, where their uptake would be influenced by soil pore water chemistry (Koritnig, 1978). This would explain the higher P background in the clay fraction. Though apatite, lazulite and wagnerite occur in hydrothermal veins, an hydrothermal origin for the P peaks at Beasley Creek is doubtful as the P peak does not occur on both sample lines. Contamination by fertilizers is unlikely at this site but the P peak is coincident with calcrete outcrops and animal burrows. The P peak in the fine soil fractions is regarded as due to localised contamination of the soil by small bone fragments, probably in goanna excrement.

S

The S distributions are similar for each size fraction, with maximum values overlying mineralisation. Sulphur is correlated strongly in the coarse fractions with As and Ba and to a lesser extent with soil pH; there are weaker correlations in all fractions with Zn. Barite ($BaSO_4$) infills small fractures in the lag at Beasley Creek (Robertson, 1989) and large crystals of gypsum ($CaSO_4.2H_2O$) have also been observed in the top metre of the weathered profile. Whether this S is derived from oxidised sulphides, or is related to geomorphology, could be pursued by a sulphur isotope study, which may still give equivocal results.

8.4 Trace Elements

The ore is clearly indicated by anomalies in Au, As, Cd Cu, Mo, Sb, Se, W and Zn. The widths of these anomalies vary from 100-900 m. Their sizes and the fractions in which they occur are summarised in Table 5. The Mo anomaly is very weak. The ore host rock is shown by maxima in Ba, Mn and possibly in Y. Lithological information may be obtained from the data for Ce, Cr, Ga, In, La and possibly Zr. Gallium and In maxima indicate the lateritic duricrust and maxima in Sr are co-located with calcrete and similar sharp increases in Ca and Mg (see Section 8.3).

The variance or geochemical 'noise' for Co, Ni, V and Y is greater over the subcrop of Archaean rocks on the hill than above the colluvium-covered, weathered, Permian glacial sediments on the flat ground to the east. Separation of the $<4\,\mu$m fraction has achieved increases in the background contents of Au, Ce, Co, La, Nb, Rb, Sn, Sr, Y and Zn but decreased the abundances of As, Bi, Cr, In and Sb. Separation of the granular 710-4000 μm fraction has achieved increases in background for Cu, Se and V.

Ag

The 'regional' and 'local' backgrounds for Ag are similar in each fraction and it does not seem to be preferentially concentrated in any of these. Though the use of ICP/MS analysis has produced smoother and presumably more reliable data, well above detection, than the XRF method used for the lags, there is no recognisable Ag anomaly. The Ag data are higher than would be expected, and the only possible interference could be from Zr (see section 4.5). However, Ag shows only a very weak correlation with Zr in the $<4\,\mu$m fraction and no significant correlation in any other fraction. Zirconium interference is therefore discounted. The fine soil fractions are slightly richer in Ag and have a slightly higher 'regional'

background than the coarse soil fractions. Correlations with other elements are all low in the coarse fractions but there is some moderate to strong correlation with Bi, In and Sn in the fine fractions.

Silver is highly mobile in the weathering environment and its precipitation conditions are different from those of Au, from which it is generally readily parted. An exception to this is under humid, neutral to alkaline conditions, when Au and Ag may be deposited together as electrum (Gray, 1988). Under the arid conditions at Beasley Creek, Ag would have been thoroughly dispersed in the saprolite. Silver is said to be adsorbed by Mn and Fe oxides and by organic matter, where it is probably chelated. Kaolinite adsorbs about twice as much Ag from aqueous solutions as ferric oxide (Vincent, 1978) but not nearly as much as manganese dioxide or freshly-precipitated ferric hydroxide. The clay-rich fractions contain slightly more Ag than the complete soil or coarse fraction. The elevated Ag concentrations in the soil at Beasley Creek, at this stage, are ascribed to adsorption by clays and iron oxides, in the absence of other, more satisfactory evidence.

As

The As data are presented in both linear and log format. There is a significant As anomaly associated with the ore host saprolite at Beasley Creek (average 42 ppm, max. 226 ppm; Robertson and Gall, 1988). In contrast, the footwall rocks average at 3.5 ppm, which corresponds with the expected background for mafic rocks. The background contents of the <75 and <4 μm fractions are similar (10 ppm) but the ferruginous 710-4000 μm fraction is elevated (60 ppm). All soil fractions show As anomalies. These are generally stronger than those found in the fine lag and, like the fine lag, are strongest on line 38940N. Anomaly to background contrasts are 2-5 and, though all the anomalies precisely define the ore position, the contrast is better in the two fine fractions, despite their lower As contents.

Arsenic is present in the cellular ironstone component of the fine lag (Robertson, 1989) and the incorporation of As into the fine fractions may reflect the friability of this component. Arsenic shows weak correlations with soil pH, Ba and Au, and, in the coarser soil fraction, with Zn.

Au

Gold has a wide range of abundance (one and a half to two orders of magnitude) so both linear and log plots are presented. Useful Au anomalies are shown by almost all the fractions. The 710-4000 μm and the <4 μm fractions have maxima of over 200 and 150 ppb respectively, whereas the <75 μm fraction shows the smallest anomaly with the least contrast. In the complete soils there is a single point anomaly of 400 ppb on line 38940N but, excluding this, the contrast is also poor. The 710-4000 μm fraction shows the strongest anomalies, over 300 m wide, with the best contrast, with very similar behaviour to that of the fine lag. These Au anomalies are asymmetrical, with wider dispersion to the east, down the steepest gradient.

The 'regional' and 'local' backgrounds in the fine lag and in the 710-4000 μm fraction are similar but this contrasts with the coarse lag. The 'local' backgrounds (50 ppb) in the fine soil fractions are significantly elevated compared to 'regional' background (5-8 ppb). This suggests a broad dispersion of Au in the clay fraction, in excess of one kilometre. The anomaly, superimposed on this elevated 'local' background, is generally less than 200 m wide and defines the ore zone well. Significant advantages may be gained from sampling the coarse, ferruginous fraction and the clay fraction. The complete soil and the <75 μm fraction, particularly if the < 4 μm fraction had been completely removed from it, are probably the least effective Au sampling media.

Gold shows moderate correlations with S, As and Mn in the 710-4000 μm fraction and in the fine fractions with soil pH, Mg, Ca (as the ore host is here fortuitously co-incident with calcrete) and As.

Ba

A distinct Ba anomaly of 1000-2000 ppm is associated with the saprolite of the ore host. This reaches 1% in one phyllitic saprolite sample. In contrast, the saprolites of the mafic footwall rocks have a range of 60-470 ppm (Robertson and Gall, 1988). This Ba anomaly is reflected by the 710-4000 μm fraction and the fine lag, which both show similar Ba peaks centred over the ore. The Ba anomalies are almost insignificant in the <75 μm and <4 μm fractions. The 710-4000 μm fraction shows a marked enhancement in background to anomaly contrast (x15) compared to the complete soil (x8).

Barium is weakly to moderately correlated with soil pH, As, Cu, Sr and Zn and strongly correlated with S in the coarse fractions and with Ti in the fine fractions. There is a strong correlation with Mn in the <4 μm fraction.

Barium has been shown to occur as barite ($BaSO_4$) in the lag. Here Ba is concentrated in the cellular ironstone and, to a lesser extent, in the red and yellow clays, but not in the calcrete component (Robertson, 1989). Barium does not seem to be related to the other group IIA elements (Mg, Ca, Sr), which appear to be related to calcrete and soil carbonate, though they have anomalies to a large extent co-located with Ba. Barium is probably present in the ore or, most likely, the ore host rock, as muscovite, prior to weathering. Any soluble Ba salts, generated by weathering, would be readily precipitated by SO_4^{2-}. While barite is important in the coarse fraction, the strong correlation with Mn suggests hollandite or (with Ca, Mg and Zn) todorokite in the fine fraction.

Be

All the Be data lie well below the ICP detection limit of 5 ppm, so the profiles only indicate geochemical noise.

Bi

No Bi anomaly has been found associated with the ore at Beasley Creek so far, however previous analyses were by XRF and only on saprolites of the ore zone. No unweathered ore has been encountered. The use of the more sensitive ICP/MS technique, instead of XRF analysis, has produced smoother data at 0.3-1.0 ppm (compare with lag data in Robertson, 1989) which are significantly above detection (0.1 ppm). In spite of this improvement there is still no apparent Bi anomaly. Bismuth correlates moderately with Cr and Sb and weakly with Mo and Pb in the coarse fractions. In the fine fractions there are moderate correlations with Ag, In, Pb and Sn. This is a typical chalcophile association with this relatively immobile element (Levinson, 1980).

Cd

All previous work at Beasley Creek (Robertson and Gall, 1988; Robertson, 1989) used XRF analysis, with detection limits of 2-5 ppm and no recognisable Cd anomaly was found. ICP/MS analysis (detection limit 0.05 ppm) used here has revealed a distinct Cd anomaly, particularly in the 710-4000 μm fraction, at below 1 ppm, with a x5 contrast and a width of 200 m. A similar but less distinct anomaly is evident in the complete soil, weakly, in the clay fraction and not at all in the <75 μm fraction. Cadmium shows moderate chalcophile correlations with Ba, Cu and Zn only in the 710-4000 μm fraction. There is weak correlation with Cr and also with Mn (probably indicating adsorption on Mn oxides) in the clay fraction.

Ce

The 'local' and 'regional' background Ce contents are similar in each soil fraction, though the Ce background contents are significantly greater in the two fine fractions. A high Ce content in the complete soil and the 710-4000 μm fraction, decreasing from west to east, probably reflects the lithological contrast between the eroded basaltic saprolite and the ore host and duricrust. The clay fraction shows a distinct decrease in Ce content over the ore host on line 38940N but, on line 38820N, this decrease occurs on the footwall. Cerium correlates consistently and moderately to strongly in all fractions with the other rare

earth elements, La and Y, as well as with Co and Mn. It also correlates moderately with Pb in the fine fractions.

Co

'Regional' and 'local' backgrounds in each size fraction are well matched but the background contents are greater in the clay fraction (24 ppm) than in the others (13-17 ppm). The complete soil and the 710-4000 μm fraction all show a significant noise level over the saprolites overlying Archaean rocks. This geochemical noise is far less on the flat ground to the east of the hill, where the soils are largely underlain by the saprolites of Permian glacial sediments. The environment provided by either the saprolites of the Permian glacial sediments, or their overlying colluvium, may have been such as to promote mobility and hence redistribution of Co. This may account for the decreased noise level in Co over the saprolitic Permian rocks. The Co content of the <75 μm and the <4 μm fractions appears to reflect the underlying lithology, being lower in Co over the ore host and higher over the mafic rocks to the east and west.

No useable ore-associated Co anomaly is apparent in the soil. The lags show a weak Co anomaly, and Co appears to be preferentially concentrated in the cellular ironstone of the lag, relative to the calcrete and red-brown clay components (Robertson, 1989). Both the Mn and Co contents are higher in the <4 μm fraction than in other fractions. Cobalt shows a weak to moderate lithophile correlation with Ce in all fractions and moderate to strong correlations with Mn and Ni in the clay fraction. It is concluded that it is probably adsorbed onto fine-grained Mn oxides among the soil clays. It is possible that a weak Co anomaly may have been present in the non-magnetic component of the 710-4000 μm fraction, if this had been collected.

Cr

Chromium is strongly concentrated in the ferruginous 710-4000 μm fraction (background 1180 ppm) relative to the two fine fractions (174-182 ppm). There is a decrease in the Cr content of the 710-4000 μm fraction over the ore host and the fine lag shows a similar response, both reflecting lithology. There is no apparent Cr response to the lithology or to the ore in the <75 and <4 μm fractions. Any chromium, which may have occurred as chromite, would have been readily removed by sedimentation, in producing the clay fraction. Remaining chromium, which forms the low background in this fraction of 180 ppm, would be chromium that was mobile in the landscape and had been adsorbed by clays and iron oxides.

Chromium correlates moderately with Bi, Ni and Sb in the coarse fraction but shows little significant correlation with other elements in the fine fractions.

Cu

The XRF data are preferred to the ICP data; the latter contain unexplained spikes. There is a moderate Cu anomaly (x2), 200 m wide, overlying the ore position in both the complete soil and in the 710-4000 μm fraction. A similar pattern is shown by the fine lag. 'Local' and 'regional' backgrounds are similar in all fractions. In the <4 μm fraction, the Cu anomaly is displaced into the footwall by about 100 m. A similar, though not very distinct, pattern is seen in the <75 μm fraction.

There are weak to moderate correlations of Cu with S, As, Au, Ba, Cd, Co, Mn, Sr, Y and Zn in the coarse fraction and with Fe, Sr, V and Zn in the clay fraction. The strongest correlations are with Zn. Many of these elements are also strongly anomalous around the ore position. Strontium follows calcrete and associated soil carbonates, which are fortuitously close to the ore, particularly on line 38940N. Copper is strongly enriched in the cellular ironstone component of the fine lag, which is also similarly enriched in As, Au, Co, Mn and Zn (Robertson, 1989). It is concluded that Cu is probably sited in the equivalent gossanous component of the 710-4000 μm fraction.

Ga

Gallium is closely associated with Al and, like Al, it is concentrated in the products of lateritic weathering. However it is more mobile than Al, so the Ga/Al ratio tends to decrease slightly where weathering is most intense. Gallium may also be associated with magnetic iron minerals (Lavrenchuk and Tenyakov, 1962, 1963; Burton and Culkin, 1978).

The highest Ga concentrations (30-40 ppm) occur in the 710-4000 μm fraction and in the <4 μm fraction. The <75 μm fraction and the complete soil contain 20-30 ppm. The maximum abundance of Ga in the complete soil and the 710-4000 μm fraction lies over the lateritic duricrust and this is similar to the response from the fine lag (Robertson, 1989). The coarse fraction shows moderate correlations of Ga with Ti and Sn so this peak does not seem to be related to the clay content. However, the fine fractions, which do not show a distinct peak over the lateritic duricrust, have Ga strongly correlated with Al and La and moderately to weakly correlated with Ce, Pb and Sn. Gallium is not regarded as ore-related but seems associated with Fe and Ti minerals in the 710-4000 μm fraction. Robertson (1989) reported a slightly enhanced Ga content in the magnetic fraction of the fine lag relative to its non-magnetic component, which is similar to the findings of Lavrenchuk and Tenyakov (1962, 1963). Gallium seems to occur with kaolinite in the soil clay fraction.

Ge

Almost all the Ge data lie below the XRF detection limit of 3 ppm and display analytical noise. A similar range of Ge data was found in the lag. Clearly a lower detection limit (1.0-0.1) would be required for meaningful results, so an improved analytical method is needed.

In

Indium, which has chalcophile and lesser siderophile characteristics, tends to be concentrated in cassiterite and chalcopyrite as well as in mica, chlorite, tourmaline and amphibole. Many igneous rocks show a correlation between Fe and In. During weathering In readily disperses, particularly under chloride-rich conditions, and precipitates with Fe oxyhydroxides and Mn oxides (Linn and Schmitt, 1978).

Long count (x7) XRF In analysis was used for the study of the lag. A large proportion of the resultant data lay at or below the detection limit of 2 ppm. Use of more sensitive ICP/MS analysis for In (detection limit 0.05 ppm) has greatly improved the quality of the soil data, which are much smoother.

There appears to be a weak In anomaly over the ore and its black shale host in the 710-4000 μm fraction but not in any other fraction. The highest In concentrations are in the 710-4000 μm fraction; the two fine fractions have less than half. Indium shows no correlations with other elements in the complete soil, weak to moderate correlations with Fe, Cd and Se in the 710-4000 μm fraction and some weak correlations with Al, Ag, Ga, Bi and Sn in the fine fractions. It is concluded that the In is largely associated with Fe oxides and oxyhydroxides in the 710-4000 μm fraction and the dispersed (chemically and/or mechanically) weak In anomaly may be reflect relict micas from the phyllitic ore host.

La

The two fine fractions are the most La rich. Both show a higher abundance of La to the east of the orebody than to the west, which is probably related to lithology. Lanthanum is strongly correlated with other rare earth elements, Ce and Y, in all fractions. In the fine fraction, La is moderately correlated with Ga, Nb, Pb and Sn and weakly with Al and Co, where it may have been precipitated and fixed, along with Al and Ga, under conditions of increased alkalinity (Herrmann, 1978).

Mn

The MnO content of some of the ore zone rocks at Beasley Creek is very high. One reaches 12.5% and several exceed 6%, so Mn is an important element in identifying the ore host. The secondary minerals,

cryptomelane and lithiophorite, have been reported from a colloform goethite-hematite rock, enclosed in ferruginised phyllitic saprolite (Robertson and Gall, 1988). Manganese can be strongly concentrated in lateritic regoliths and, here, the underlying phyllite was probably enriched in Mn. Manganese minerals commonly have a variety of trace elements either adsorbed onto their surfaces or co-precipitated with them.

Both linear and log plots are provided of the ICP and XRF data, which are in close agreement. There is a marked Mn anomaly which covers the orebody, its phyllitic host, the lateritic duricrust and the eastern flank of the hill in all soil fractions. This is strongest on line 38820N and is similar in width and strength to that found in the lag (Robertson, 1989) but the range is smaller. The contrast and width of the Mn anomaly is greater in the $<4\,\mu$m soil fraction than in the 710-4000 μm fraction. 'Regional' and 'local' backgrounds are similar for all fractions.

Only Ce, Co and Zr are weakly correlated with Mn in the complete soil. Manganese correlates moderately with Au in the 710-4000 μm fraction and there are also weak correlations with Fe, As, Cu and Zn. The $<75\,\mu$m fraction shows moderate Mn correlations with Ce and Co. The $<4\,\mu$m fraction shows weak Mn correlation with Bi, Cd, La, Pb and Sn, and moderate to strong correlations with Ba, Ce and Co. Manganese anomalies are related to the ore host rock.

Mo

Weak anomalies were noted in the lag and one sample in the phyllitic saprolite host has a single point anomaly of 23 ppm in a background of 0-5 ppm (Robertson, 1989; Robertson and Gall, 1988). Molybdenum is mobile under oxidising, alkaline conditions but it is readily precipitated in the presence of Pb (wulfenite, $Pb[MoO_4]$), Fe (ferrimolybdite, $Fe_2[MoO_4]_3.7H_2O$) and Ca (powellite, $Ca[MoO_4]$) (Levinson, 1980).

The Mo data all lie very close to the detection limit (5 ppm) but the 710-4000 μm fraction data are slightly less noisy compared to the fine lag, suggesting either an improvement in the INAA analytical quality or a more consistent sampling medium. The Mo levels in each soil fraction are similar. Though the 'local' and 'regional' background levels are also similar (3.4-4.7 ppm), the range of the Mo content of the 710-4000 μm fraction (7 ppm) is greater than in any other soil fraction (1-2 ppm). The 710-4000 μm fraction and the two fine fractions appear to show a weak anomaly over or very close to the orebody. This is not clearly apparent in the complete soil. Molybdenum shows moderate correlations in the complete soil with Fe, Pb, Sb and V and weak correlation with Bi, Se and V in the 710-4000 μm fraction. In the fine fractions Mo shows no significant correlation with other elements. An improved analytical technique would be necessary to investigate the performance of Mo satisfactorily, though the results are encouraging.

Nb

The complete soil, the lag and the 710-4000 μm fraction are all comparatively poor in Nb, compared to the clay-rich fine fractions, and the data lie close to the XRF detection limit (5 ppm). The higher Nb concentration in the soil clay fraction is matched by a high Nb abundance in the 'regional' background. Niobium has been found to be enriched in the khaki lag and in the associated red-brown clays, from which much of the soil clays are probably derived. Though much of the data lie close to the detection limit, several of the plots indicate some Nb depletion over the ore position.

Niobium shows little correlation in the coarse fractions but is moderately correlated with Ti, La and Pb and weakly correlated with Y and Zr in the fine fractions. Apart from forming its own minerals (columbite and pyrochlore), generally immobile Nb is also found in pyroxene, amphibole, biotite, muscovite, magnetite and is often contained in the Ti minerals, sphene, ilmenite, titano-magnetite, rutile, brookite and pervoskite as well as in Zr minerals (Heinrich, 1978). At Beasley Creek, it is probably

present in very fine-grained detrital rutile and zircon, in the fine fraction of the soil, in which it has been slightly enriched.

Ni

Both the ICP and the XRF data are moderately well correlated, particularly in the finer fractions. The XRF data are slightly smoother and are preferred. The ICP Ni data tend to be systematically high in the 710-4000 μm fraction but the ICP and XRF data compare closely in the two fine fractions, suggesting some ICP interference from Fe.

The highest Ni concentrations occur in the <4 μm fraction and, to a lesser extent, in the 710-4000 μm fraction. A slightly higher Ni content occurs over the mafic rocks to the west of the hill and the Ni variance is high compared to that over the Permian rocks to the east. Nickel is slightly depleted in the 710-4000 μm fraction over the lateritic duricrust. The highest Ni concentrations occur in the red-brown clays of the lag (Robertson, 1989), indicating significant Ni mobility in the ferruginous rocks at the top of the lateritic profile, where Ni is known to be mobile under acidic, oxidising conditions.

Nickel is only weakly to moderately correlated with Cr and Sb in the coarse fractions. In the fine fractions it is weakly correlated with Fe, Co, Cu and Rb and the <75 μm fraction, it is strongly correlated with Al and Ga and moderately correlated with Sn. Nickel is probably sited in lithorelics in the 710-4000 μm fraction and in the lag, where it is still, in part, immobile, related to the underlying rock type and is still correlated with Cr. In the fine soil fractions this nexus is broken, the Ni has been mobile and is probably now adsorbed on Fe oxides and clays, giving the observed correlations with Fe, Ga and Al. Like Co, it is not related to ore but, in part, to the underlying rock type in the coarse soil fractions. The degree of localised variance (noise) for Ni appears to differentiate between underlying Archaean and Permian rocks.

Pb

'Regional' and 'local' background concentrations for Pb are similar in each fraction and the fractions themselves are very similar in their Pb content (20-30 ppm). The coarse lag showed a localised anomaly close to the ore on both lines, at one point reaching 120 ppm compared to a background of 50 ppm. This was not reflected in the fine lag or in any of its sub-fractions (Robertson, 1989). Although there is a weak Pb anomaly in the saprolitic ore host (Robertson and Gall, 1988), caution was considered necessary in interpreting the lag anomaly in view of its proximity to town and to the main road, at a position where rabbit burrows abound in the surrounding calcrete.

There are no distinguishable Pb anomalies in any of the corresponding soil fractions. The range in Pb content of the 710-4000 μm fraction (20 ppm) is similar to that in the lag (exclusive of the anomaly). Since the soil samples were collected from beneath the lag, it is concluded that the lag Pb anomaly is probably due to a smear of lead shot on a coarse lag fragment (ballistic contamination).

The coarse fractions show only weak correlations of Pb with Fe, Bi, Sb and V. The fine fractions show that Pb correlates weakly with Sn, moderately with Bi, Ce, Ga and Nb, and strongly with La and Y. This is not a typical chalcophile association so Pb does not seem to be important as an indicator of ore in the surface materials at Beasley Creek.

Rb

Rubidium is concentrated in K-bearing minerals, K-feldspar and mica. Higher levels of Rb may be expected in shales and in granites than in mafic and ultramafic rocks. The Rb levels in the fine soil fractions, and particularly in the <4 μm fraction, are significantly higher than those encountered in the 710-4000 μm fraction and in the coarse and fine lag. The Rb content in the fine fractions is not

apparently due to sericite, as the Rb and sericite do not appear to be correlated and neither is it due to feldspar (Section 7.2).

Rubidium shows weak to moderate correlations with a number of elements but there is little commonality between fractions. In the complete soil it is moderately correlated with Nb and Sn, in the 710-4000 μm fraction it is moderately correlated with Mg and Na. The <75 μm fraction shows moderate correlation of Rb with Al, Ga, Ni and Sn and the <4 μm fraction shows only weak correlation with Fe, Cu, Nb, Ni and Zn.

Sb

The 710-4000 μm fraction shows a very similar Sb anomaly to the fine lag in both size (5-6 ppm) and background (3 ppm). However, the range in 'regional' background is slightly greater than that encountered in the fine lag, so the anomaly is not quite as distinctive. There is a similar Sb anomaly in the saprolitic ore host of 8 ppm in a background of 3 ppm (Robertson and Gall, 1988). The cellular ironstone component of the fine lag and the 710-4000 μm fraction carries the anomalous Sb geochemical signal (Robertson, 1989). The Sb contents of the two fine fractions are considerably lower (1 ppm or less) and there is no distinctive anomaly.

In the coarse fraction, Sb shows strong correlation with Cr, moderate correlations with Bi and Ni and weak correlations with Co and Pb; correlations are all weak in the fine fractions. Antimony is relatively immobile in the secondary environment (Levinson, 1980) but it is interesting to note that the Sb levels in soils are considerably higher than those which would be expected from igneous rocks (Onishi, 1978).

Se

Most of the Se is in the ferruginous 710-4000 μm fraction, which shows an anomaly over the ore position on line 38820N and to the east of the ore on line 38940N. This is very indistinct in the complete soil and not distinguishable at all in the two fine fractions, where most of the data lie below the detection limit. Similar Se anomalies were found in the coarse lag, the fine lag and specifically in its non-magnetic component. The cellular ironstone carries the Se geochemical signal (Robertson, 1989). Selenium shows moderate correlation with Fe, Ti and V in the 710-4000 μm fraction; all other correlations are weak and inconsistent between fractions. Selenium-bearing sulphides are readily oxidised and the resultant selenite ions are stable and migrate until adsorbed by iron hydroxides where they are nearly quantitatively fixed in the "iron cap" (Leutwein, 1978). It appears that Se adsorption by clays in the soils at Beasley Creek is minimal, most of it being fixed by adsorbtion onto Fe oxyhydroxides in the 710-4000 μm fraction.

Sn

Though there appeared to be a weak Sn anomaly in the fine lag, it was not reproduced in any of its components and much of the data were at or below the detection limit of 2 ppm (long count XRF). Consequently Sn was determined on the soil by ICP/MS analysis, with a detection limit of 0.1 ppm. This confirmed a 2 ppm background, gave much smoother results but, despite better data, there is no useful Sn anomaly apparent in any of the soil fractions. The Sn background content of the fine fractions, particularly the <4 μm fraction, is significantly higher (3-6 ppm) than those of the 710-4000 μm fraction and the complete soil (1.0-2.5 ppm). Tin shows moderate correlations with Al and Ga and weak correlations with In and La in most fractions. The fine fractions show moderate to strong correlations with Ag and weak correlations with Bi, Ce and Pb. There are two mechanisms by which Sn could be concentrated in the fine soil fraction, either by adsorption onto clays, or by inclusion of trace quantities of resistant, detrital Sn minerals. In the former mechanism the soluble, but far too readily oxidised, Sn^{2+} ion would be needed to transport Sn. In the latter mechanism the dense, detrital Sn minerals would have to be extremely fine-grained in order to achieve hydraulic equivalence to 2-4 μm clays during clay separation.

Sr

All lag fractions show a marked Sr maximum closely associated with the ore position. The strongest peak is found on line 38940N where calcrete outcrops. Almost identical strong Sr maxima are found in the complete soil and the 710-4000 μm fraction. The Sr peak is still apparent in the <74 μm fraction but only weakly present in the <4 μm fraction.

There is no ore-associated Sr anomaly in the saprolite (Robertson and Gall, 1988). The lag study clearly demonstrated that Sr occurs in calcrete fragments, the presence of which cause similar and coincident peaks in Ca and Mg (Robertson, 1989). The mineralogical study of the soil showed that calcite is present where there is an enrichment in Ca, Mg and Sr, where its presence is reflected by a high soil pH. Calcite was not detected in the <4 μm fraction and this may reflect the coarser particle size of calcite. Very fine-grained calcite, however, would be rendered soluble by the HCl, added to flocculate the clays at pH 4.0 (see Section 4.3). It is interesting to note that the overall Sr background is higher in the fine soil fractions by a factor of about five. 'Regional' and 'local' backgrounds are remarkably similar in all soil fractions.

Strontium is strongly correlated with soil pH, Mg and Ca in all soil fractions, except in the clay fraction, where the correlation is much weaker. All soil fractions show weak correlations of Sr with Cu. The coarse fractions show moderate correlations with Na and this is strong in the clay fraction. The Sr content of the coarse soil fractions appears to be related to the content of soil carbonate. It seems that the elevated Sr background in the <4 μm fraction is not related to carbonate but possibly to very fine-grained detrital feldspar, which would explain the correlation of Sr with Na. It is unlikely that any alkali or alkaline earth chlorides would be present in the <4 μm fraction, in view of the aqueous method of clay separation.

V

The ICP data are significantly and systematically lower than the XRF data for V in the 710-4000 μm fraction. Similar systematic differences were found in the lag samples but these differences are far less apparent in the complete soil, which suggests that interference from iron is probably the cause. The data from the two methods are very strongly correlated.

Vanadium minerals (mafic minerals, muscovite, magnetite and ilmenite) are relatively easily weathered and V is mobile under a variety of oxidising acid to alkaline conditions but it is readily adsorbed by Mn and Fe oxides. Vanadium contents of the phyllitic ore host rock and its footwall are of the order of 500-700 ppm (Robertson and Gall, 1988) except near the iron-rich top part of the profile where it reaches over 1300 ppm. While there is no V anomaly related to the ore position, the variance in the V data is higher over the hill than on the flat ground to the east. 'Regional' and 'local' backgrounds are consistent in each fraction but the fine fractions are very poor in V relative to the 710-4000 μm fraction.

Vanadium is strongly correlated with Fe in all fractions, which suggests that V is adsorbed by, or was co-precipitated with, the iron oxyhydroxides. In the coarse fractions it is also weakly correlated with Mo, Pb and W and moderately with Ti. The fine fractions show a strong correlation of V with Cu.

W

'Regional' and 'local' background W abundances are consistent and are very similar for all soil fractions. The fine lag and the 710-4000 μm fraction show very similar W anomalies of 6-8 ppm compared to a background of 2-3 ppm in the footwall and over the lateritic duricrust. The ore host contains a distinct W anomaly of 30-55 ppm over a background of 3-10 ppm, in the footwall rocks (Robertson and Gall, 1988). There is no clear anomalous behaviour in the <75 μm fraction, but the <4 μm fraction is weakly anomalous on line 38820N near the ore and in the hangingwall. Most of the background data are at or slightly above the INAA detection limit of 2 ppm.

Tungsten correlates with Fe, Ti, S, V and Y in the complete soil, with Fe, Ti, Au, Ga, Mn, Se and V in the 710-4000 μm fraction. It shows little significant correlation in the fine fractions. The correlation with Fe and the slightly elevated W background in the 710-4000 μm fraction, where it has formed a fairly broad anomaly (100-300 m), suggests that the W is not detrital but has been made soluble by weathering and may have been deposited with Fe oxyhydroxides as some form of tungstic oxide (see Krauskopf, 1978) in the 710-4000 μm fraction. The narrower dispersion in the <4 μm fraction may be due to detrital W.

Y

In the 710-4000 μm fraction, the 'regional' and 'local' background contents are consistent and are similar to those encountered in the fine lag. Though there is a slightly increased variance in the Y data over the hill, as in the fine lag, there is no detectable Y anomaly. The 'regional' and 'local' backgrounds are significantly increased in the finer fractions and particularly so in the <4 μm fraction, which shows a dip in Y levels over the ore host and a small anomaly over the lateritic duricrust.

Yttrium correlates moderately to strongly with La in all fractions, particularly in the fine fractions, and weakly with Ce. In addition, the fine fractions show moderate to strong correlations with Pb and weak to moderate correlations with Nb.

Zn

The 'local' and 'regional' background abundances for Zn are consistent in all fractions, though the Zn background is significantly elevated (x2) in the <4 μm fraction. There is a very clear and broad Zn anomaly related to the ore in the 710-4000 μm fraction and this is also present in the fine lag and particularly in its non-magnetic component, where the cellular ironstone is regarded as the host (Robertson, 1989). The Zn anomaly appears to be slightly broader, though less distinct in the fine fractions, though a single sample shows a spot high on line 38940N.

There is a x3 Zn anomaly (320 ppm over a background of 100 ppm) associated with the ore saprolite at Beasley Creek (Robertson and Gall, 1988). The Zn background (50 ppm), the Zn anomaly (100 ppm) and the anomaly contrast are lesser in the soil, but the anomaly is wide (200 m). This reflects the mobility of Zn during weathering, where it is soluble under oxidising, acid to neutral conditions and is readily adsorbed by Fe oxyhydroxides. Zinc is moderately correlated with soil pH and moderately to strongly correlated with Cu in all fractions.

Zr

Zirconium, where it occurs as zircon, is generally very stable and concentrates as a resistate mineral. Where it occurs in other minerals, replacing Ti, Nb, Ta, REE, Fe and Ca, it is less stable and weathers with these minerals. Even zircon may be corroded by carbonate-rich or acid groundwaters and the stability of zircon may be significantly reduced if its lattice is damaged (metamict) by radiation. Dissolved zirconium may be fixed by clays or hydrolysed to colloidal particles (see Erlank *et al*, 1978).

The 'regional' and 'local' Zr background levels are consistent for each soil fraction and all are similar except for the <75 μm fraction, which is significantly elevated (x2.5). This is most likely due to the presence of tiny zircons, so providing further evidence for aeolian transport of the intermediate to moderately fine fractions of this soil. There is no ore-related Zr anomalies but Zr is preferentially enriched in the red-brown clays in relation to the cellular ironstone (Robertson, 1989).

In the soils at Beasley Creek, Zr shows little consistent correlation with other elements apart from a strong correlation with Ti and a moderate to strong correlation with Nb in the fine fractions.

9.0 CONCLUSIONS

9.1 Soil Geology and Composition

The low hill at Beasley creek is almost completely mantled by 100-500 mm of residual soil, which is thinnest near the top of the hill. The soil is alkaline, near where calcrete subcrops at the top of the hill; elsewhere the soil is neutral to acid. The base of the soil is marked by hardpan or in places by saprolite or calcrete.

The soil consists of a mixture of three contrasting fractions. The coarse fraction (>710 μm) is comprised of dense, goethitic as well as slightly less-dense, ferruginous, clay pebbles and granules, with a few quartz grains, fragments of calcrete and hardpan. The intermediate fraction (75-710 μm) consists largely of hematite-coated, wind-blown quartz sand, with minor grains of feldspar, and small ferruginous granules. The fine fraction (<75 μm) consists of quartz grains and smaller kaolinite and iron oxide particles (<1 μm).

The coarse fraction appears to have been derived from the underlying saprolite. The intermediate fraction appears to be a largely dynamic, aeolian component, which acts as a diluent to the coarse fraction. Possible sources for this aeolian sand , at decreasing distances from the Beasley Creek Mine Site, are; the sand dunes covering the sand plains which overlie granitic terrain (5 km), sand-filled fluvial channels (e.g. the Beasley Creek; 1-2 km) and the adjacent tracts of Wanderrie Country (0.5 km). Any settled, wind-blown material would be incorporated into, and mixed with, the soil by pedoturbation and illuviation processes. The fine fraction was probably, in part, locally derived, by mechanical breakdown of clay pisoliths and granules, and, in part, wind-blown; geochemical evidence suggests that input from the latter was minimal. Later deflation of the upper soil layers, by wind and water, left a discontinuous desert armour of lag.

The ferruginous granules of the coarse fraction are petrographically indistinguishable from those of the fine lag, for which they provided the source. They consist of black, nodular, goethitic granules, some of which are magnetic, red to yellow, ferruginous, clay-rich granules, quartz fragments and rare, cellular, gossan fragments. The proportion of gossan fragments is significantly greater close to the orebody. Petrography of the interiors of the goethitic granules reveal mica relics and goethite pseudomorphs after kaolinitic lithorelics, as well as vermicular accordion structures, all set in a variety of secondary goethite (massive, spongy, vesicular, colloform). The clay-rich granules show several generations of clay and permeation and sealing by even later goethite. The gossan fabrics suggest derivation from pyrrhotite, marcasite, chalcopyrite and galena. Study of the lag suggest that most of the geochemical signal is contained in the gossan component, so it is reasonable to suppose that this is equally true of the 710-4000 μm fraction.

9.2 Mineralogy

The mineralogy of the complete soil shows it is a relatively simple mixture. *Quartz* occurs as fragments of vein quartz but dominantly as wind-blown sand. *Kaolinite* forms loose clay-sized particles but also forms a component of coherent clay pisoliths and granules. The iron oxides, *hematite and goethite*, form loose, clay-sized particles, occur as major components of black, dense granules and form minor components of clay-rich granules. They also coat sand grains. *Sericite* occurs as a component of some ferruginous, granular lithorelics and as small, loose flakes approaching the size of clay particles. *Feldspar*, chiefly unweathered microcline and microcline perthite, occurs as part of the wind-blown sand component. *Rutile* forms a minor component of the ferruginous 710-4000 μm fraction. *Calcite* occurs as minor, coarse calcrete fragments and as small sand- and silt-sized particles.

The effect of fractionation of the soil into the 710-4000, <75 and <4 μm size fractions has been to yield a fraction rich in the iron oxides (710-4000 μm) which has considerable value as a geochemical sampling medium because of its adsorptive characteristics. Quartz and feldspar are concentrated in the <75 μm fraction and even more so in the discarded 75-710 μm fraction, which contains the bulk of the diluting aeolian material. Kaolinite is concentrated in the <75 μm fraction and particularly in the <4 μm fraction. Kaolinite and adhering iron oxides also have adsorptive properties. Calcite occurs in all fractions, except for the <4 μm fraction from which it has been largely eliminated by acidification of the clay suspension.

Smoothed plots of kaolinite and sericite abundances show maxima, 200-300 m wide, located over the ore. This is most clearly shown by the <4 μm fraction. These maxima are probably related to the phyllitic nature of the host rocks, in contrast to the surrounding mafic and ultramafic lithologies.

9.3 Geochemistry

Geochemical background has been established using four samples collected about 600 - 700 m north and south of the centre of the pit. This background geochemical information has been reinforced by extending the two soil sample lines about 800 m east from the centre of the pit. Though these sample sites overlie a variety of lithologies, they have proved valuable as a background reference.

Extraction of the fine fraction has increased the levels of abundance of Si, Al, Mg, Ti, Au, Ce, Co, La, Mn, Nb, Ni, Rb, Sn, Sr, Y, Zn and decreased the contents of Fe, As, Cu, Cr, In, Sb, Se, V and W in relation to the coarse fraction. The geochemical characteristics of the 710-4000 μm fraction and the fine lag are identical, which is to be expected as the latter was derived from the former.

Apart from Au, the orebody and its host are depicted by soil anomalies in the chalcophile elements As, Cd, Cu, Sb, Se and Zn and the lithophile elements Ba, Mn and W. Silicon shows a decrease over the ore host and the lateritic duricrust and Fe shows a complementary increase. Gold is the most distinctively anomalous element, giving a very broad peak of >20 ppb but locally reaching 200-300 ppb. The 710-4000 μm fraction is the most effective medium for Au, giving the highest values and the greatest anomaly to background contrast. Anomalies, their sizes and the fractions in which they occur are compared in Table 5.

Increased geochemical noise in Co, Ni and V over the hill at Beasley Creek reflects the saprolites of Archaean rocks buried under a shallow, residual soil. This may be contrasted with the lesser geochemical noise in these elements, over weathered Permian rocks, possibly buried under a slightly deeper, colluvial soil.

Coincident peaks in Ca, Mg and Sr in all fractions are related to the occurrence of soil carbonates and calcrete. Though these are co-located with the ore host at the top of the hill at Beasley Creek, these localised increases are most likely related to the landscape. Small nearby peaks in P in the complete soil and the <75 μm fraction are probably related to small bone fragments, scattered from the excrement from goanna burrows under the calcrete. Though a small Pb anomaly was reported in the coarse lag from a similar locality by Robertson (1989), there was no corresponding anomaly in the fine lag. The soil also shows no Pb anomaly, so contamination of the lag sample by shotgun pellets is possible.

As in the lag, the signature of the phyllitic ore host rock is shown by increased concentrations of Ba and Mn. Manganese enrichment occurs in all fractions but Ba occurs mainly in the 710-4000 μm fraction. Sulphur is also anomalous in all fractions. Both gypsum and barite occur at Beasley Creek but the principal host minerals and origins of the sulphur have not been established.

Anomalies in As, Au, Cd, Cu, Sb, Se, W and Zn are considered to be ore-related. Though As is concentrated in the 710-4000 μm fraction, better anomaly/background contrast is to be found in the fine fractions. ICP/MS analyses, with lower detection limits for Ag, Bi, Cd, In and Sn only showed a significant anomaly for Cd. The Cd anomaly is best shown by the 710-4000 μm fraction and has a higher contrast (x6) than the equivalent Zn anomaly (x2), though Zn is more abundant by two orders of magnitude.

9.4 Exploration Implications

* Gold anomalies, and particularly their contrast, are greatly improved by the use of the course, ferruginous 710-4000 μm fraction, in preference to the complete soil.

* The much broader dispersion of Au, compared to other elements, showed by an elevated 'local' background over about a kilometre, suggests that Au has been chemically dispersed in the regolith prior to mechanical dispersion at surface. In some instances this greatly enhances its usefulness but great care is necessary in establishing geochemical background and in ensuring analytical control. In other instances this enhanced Au mobility could lead to loss of the Au anomaly and the multi-element signature then takes on greater importance.

* The enhanced dispersion of Au in the clay fraction, together with proven responses in As, Cd and Cu, suggests that it could be used for drainage surveys in areas of low relief. Its separation from the soil does not present any great technical difficulties (see Figure 3B).

* Apart from Au, anomalies in As, Cd, Cu, W and Zn make up the multi-element signature of Beasley Creek.

* The anomalies in Au, and in other pathfinder elements, appear not to have been aberrated by the aqueous chemistry of the clay sedimentation technique or the pH control (4.0-8.0) required to disperse and flocculate the clays. This technique is a useful tool for separating the clay fraction for multi-element geochemistry.

* The largely wind-blown, quartz-rich 75-710 μm fraction acts as a diluent and, where this occurs in a soil, it should be removed, by sieving, prior to analysis. The value of size fractionation and microscopic examination of a soil, during an orientation study, cannot be overemphasised.

* The $<4\,\mu$m fraction is preferable to the $<75\,\mu$m fraction as the latter also contains a wind-blown component.

* Tungsten, which generally is resistant and is not readily dispersed, shows evidence of a slightly broader dispersion in the iron-rich material than would normally be expected from mechanical dispersion alone.

TABLE 5

	Complete Soil		710-4000 µm		<75 µm		<4 µm		
	Peak Type	Width (m)	Peak Type	Width (m)	Peak Type	Width (m)	Peak Type	Width (m)	Possible Source
SiO2	-		U	400	-		-		
Al2O3	-		-		-		U	200	
Fe2O3	-		M	400	-		-		
MgO	Δ	100	Δ	100	Δ	100	Δ	100	Calcrete
CaO	Δ	100	Δ	100	Δ	100	Δ	100	Calcrete
TiO2	-		-		-	200	-		
S	√	300	√	300	√		√	200	?
Na2O	-		-		-		-		
P2O5	-		-		-		-		
Ag	-		-		-		-		
As	√	100	√	200	√	100	√	100	Ore
Au	√	900/200	√	300	√	900/100	√	900/200	Supergene
Ba	√	200	√	300	?		?		Ore Host
Be	-		-		-		-		
Bi	-		-		-		-		
Cd	√	300		200	?		√	100	Ore
Ce	-		-		-		-		
Co	-		?		-		-		
Cr	U		U	400	-		-		
Cu	√	200	√	200	-		√	200	Ore
Ga	-		-		-		-		
Ge	-		-		-		-		
In	-		?	400	-		-		
La	-		-		-		-		
Mn	√	300	√	200	√	300	√	300	Ore Host
Mo	-		?		?		?		Ore
Nb	-		-		-		-		
Ni	-		-		-		-		
Pb	-		-		-		-		
Rb	-		-		-		-		
Sb	√	200	√	200	-		-		Ore
Se	√	200	√	300	-		-		Ore
Sn	-		-		-		-		
Sr	Δ	1-200	Δ	1-200	Δ	200	-		Calcrete
V	-		-		-		-		
W	?	100	√	200	?		√	200	Ore
Y	-		-		U	150	U	150	Ore Host
Zn	√	200	√	200	√	200	√	200	Ore
Zr	-		-		-		-		

√ Ore- or Ore Host-related Anomaly
Δ Calcrete-related Maximum
U Broad decrease over Ore Host
M Broad maximum over Ore Host
? Indistinct feature

10.0 ACKNOWLEDGEMENTS

H.M. Churchward and L.M. Lawrance assisted with soil sampling. Sample preparation was largely by R.J. Bilz, with assistance by J.D.S. Wass, and G.D. Longman, though the author must take responsibility for soil fractionation. In-house XRF geochemical analyses were performed by M.K.W. Hart, and the ICP analyses by J.E. Wildman and G.D. Longman. INAA analysis was by Becquerel Laboratories at Lucas Heights and ICP/MS analysis by Analabs in Perth. XRD data for the larger data set were collected by M.K.W. Hart and G.D. Longman, those for the smaller data set were collected by A.R. Horne and interpreted by G.F. Taylor. Thin and polished sections were prepared by A.G. Bowyer. Assistance on the SEM was ably given by G. Burkhalter. Advice on dispersion, fractionation and flocculation of clays was given by P. Darragh, C. Foudoulis (ANU), D.J. Gray and P. Shawcross. H.M. Churchward provided additional geomorphological input. Drafting and artwork was by A.D. Vartesi; J.J. Porter and C.K. Harris checked and formatted the final document. Western Mining Corporation Ltd., assisted with accommodation and logistics while at Laverton. All this is acknowledged with appreciation. Thanks also goes to C. Reddell and J. Hronsky who provided assistance at Beasley Creek and to C.R.M. Butt and R.E. Smith who provided critical comment on the manuscript.

11.0 REFERENCES

Brindley, G.W. 1980. Quantitative X-ray mineral analysis of clays. in G.W. Brindley and G. Brown (eds). Crystal structures of clay minerals and their X-ray identification. Mineralogical Society Monograph No 5. 411-438.

Burton, J.D. and Culkin, F. 1978. Gallium. in K.H. Wedepohl (ed). Handbook of Geochemistry. Springer-Verlag. New York.

Erlank, A.J., Smith, H.S., Marchant, J.W., Cardoso, M.P. and Ahrens, L.H. 1978. Zirconium. in K.H. Wedepohl (ed). Handbook of Geochemistry. Springer-Verlag. New York.

Gray, D.J. 1988. The aqueous chemistry of gold in the weathering environment. CSIRO Division of Exploration Geoscience, Restricted Report 4R, 65 pp.

Hart, M.K.W. 1989. Analysis for total iron, chromium, vanadium and titanium in varying matrix geological samples by XRF, using pressed powder samples. Standards in X-ray analysis. Australian X-ray Analytical Association (WA Branch) Fifth State Conference. 117-129.

Heinrich, E.W. 1978. Niobium. in K.H. Wedepohl (ed). Handbook of Geochemistry. Springer-Verlag. New York.

Herrmann, A.G. 1978. Yttrium and lanthanides. in K.H. Wedepohl (ed). Handbook of Geochemistry. Springer-Verlag. New York.

Holmes, A. 1944. Principles of physical geology. Thomas Nelson and Sons Ltd. London. 532 pp.

Koritnig, S. 1978. Phosphorus. in K.H. Wedepohl (ed). Handbook of Geochemistry. Springer-Verlag. New York.

Krauskopf, K.B. 1978. Tungsten (Wolfram). in K.H. Wedepohl (ed). Handbook of Geochemistry. Springer-Verlag. New York.

Lavrenchuk, V.N. and Tenyakov, V.A. 1962. Distribution of gallium in bauxites. Geochemistry (USSR) p 862.

Lavrenchuk, V.N. and Tenyakov, V.A. 1963. Gallium balance in bauxites. Dokl. Akad. Nauk SSSR 151, 1430; Chem. Abstr. 59, 15069f.

Leutwein, F. 1978. Selenium. in K.H. Wedepohl (ed). Handbook of Geochemistry. Springer-Verlag. New York.

Levinson, A.A. 1980. Introduction to exploration geochemistry - the 1980 supplement. Applied Publishing Ltd. Wilmette. 924 pp.

Linn, T.A. (Jr.) and Schmitt, R.A. 1978. Indium. in K.H. Wedepohl (ed). Handbook of Geochemistry. Springer-Verlag. New York.

Mabbutt, J.A. 1963. Wanderrie banks: micro-relief patterns in semiarid Western Australia. Geol. Soc. Amer. Bull. 74. 529 - 540.

McDonald, R.C., Isbell, R.F., Speight, J.G., Walker, J. and Hopkins, M.S. 1984. Australian soil and land survey. Inkata Press, Melbourne. 160 pp.

Norrish, K. and Chappell, B.W. 1977. X-ray fluorescence spectrometry. in J. Zussman (ed). Physical methods in determinative mineralogy. Academic Press, London. 201-272.

Onishi, H. 1978. Antimony. in K.H. Wedepohl (ed). Handbook of Geochemistry. Springer-Verlag. New York.

Robertson, I.D.M. 1989. Geochemistry, petrography and mineralogy of ferruginous lag overlying the Beasley Creek Gold Mine - Laverton, WA. CSIRO Division of Exploration Geoscience, Restricted Report 27R, 180 pp.

Robertson, I.D.M. and Churchward, H.M. 1989. The pre-mining geomorphology and surface geology of the Beasley Creek Gold Mine, Laverton, WA. CSIRO Division of Exploration Geoscience, Restricted Report 26R, 39 pp.

Robertson, I.D.M. and Gall, S.F. 1988. A mineralogical, geochemical and petrographic study of rocks of drillhole BCD1 from the Beasley Creek Gold Mine - Laverton, WA. CSIRO Division of Exploration Geoscience, Restricted Report MG 67R, 44 pp.

Vincent, E.A. 1978. Silver. in K.H. Wedepohl (ed). Handbook of Geochemistry. Springer-Verlag. New York.